

ON RANDOM CLASSICAL MARGINAL PROBLEMS WITH APPLICATIONS TO QUANTUM INFORMATION THEORY

ANKIT KUMAR JHA AND ION NECHITA

ABSTRACT. In this paper, we study random instances of the classical marginal problem. We encode the problem in a graph, where the vertices have assigned fixed binary probability distributions, and edges have assigned random bivariate distributions having the incident vertex distributions as marginals. We provide estimates on the probability that a joint distribution on the graph exists, having the bivariate edge distributions as marginals. Our study is motivated by Fine’s theorem in quantum mechanics. We study in great detail the graphs corresponding to CHSH and Bell-Wigner scenarios providing ratios of volumes between the local and non-signaling polytopes.

CONTENTS

| | |
|---|----|
| 1. Introduction | 1 |
| 2. The classical marginal problem | 4 |
| 3. Slices of the correlation polytope | 5 |
| 4. Relation to quantum information theory and contextuality | 8 |
| 5. Random marginal problems | 11 |
| 6. The triangle graph | 12 |
| 7. The square graph | 20 |
| 8. Cycle graphs | 25 |
| 9. The complete graph on four vertices | 27 |
| 10. Operations on general graphs | 30 |
| 11. Conclusion | 36 |
| References | 37 |
| Appendix A. Graphs and Plots | 38 |

1. INTRODUCTION

Alongside quantum entanglement, quantum nonlocality is one of the main features of quantum theory that sets it apart from classical mechanics. It is the principle that some statistics observed in quantum experiments do not allow for a local realistic explanation. Arguably one of the most impactful developments in the foundations of quantum theory, nonlocality is often modeled in terms of *Bell inequalities* [Bel64, CHSH69], mathematical relations that impose bounds on the correlations that can be explained by local theories; these inequalities have been experimentally violated, excluding local hidden variable models as possible theories explaining Nature [AGR82, HBD⁺15]. Violations of Bell inequalities show that quantum correlations that can be obtained in some experimental setting contain as a *strict* subset classical correlations. Importantly, Popescu and Rohrlich introduce a superset of correlations, called *non-signaling*, that obey the principle from special relativity that no faster-than-light communication is allowed. These non-signaling correlations [PR94] form a strict superset of quantum correlations. Understanding how the three sets of classical, quantum, and non-signaling correlations that can be obtained in a given setting is a central problem in the foundations of quantum theory [BCP⁺14, Sca19].

This work continues this line of investigation by analyzing the containment of the set of local correlations inside the set of non-signaling correlations, in various scenarios encoded by graphs. We connect the problem of computing the ratio of the volumes of these two convex sets (which are polytopes) to two other mathematical problems and, using this connection, we provide exact computations in various specific and general scenarios. The volume of the classical (\mathcal{L}), quantum (\mathcal{Q}), and non-signaling (\mathcal{N}) sets of correlations in the setting of the CHSH game have been computed in [Cab05]:

$$\text{vol}(\mathcal{L}) = \frac{2^5}{3} < \text{vol}(\mathcal{Q}) = \frac{3\pi^2}{2} < \text{vol}(\mathcal{N}) = 2^4,$$

which leads to a ratio of

$$\frac{\text{vol}(\mathcal{L})}{\text{vol}(\mathcal{N})} = \frac{2}{3}.$$

Further research on the relative volume of classical and quantum correlations have been performed with the help of the tensor norm formalism in [GGLPV17, DBAC18].

In this work, we shall focus not on the set of correlations itself, but on the set of conditional probabilities (sometimes called behaviours) that yield the correlations in a Bell scenario: $\mathbb{P}(a, b|x, y)$. The non-signaling condition, which is satisfied by both classical and quantum strategies, states that the marginal distribution with respect to one party should be independent of that party's question:

$$\begin{aligned} \sum_b \mathbb{P}(a, b|x, y) & \text{ does not depend on } y \\ \sum_a \mathbb{P}(a, b|x, y) & \text{ does not depend on } x. \end{aligned}$$

In other words, one can define marginal distributions $\mathbb{P}(a|x)$ and $\mathbb{P}(b|y)$. We propose in this work an analysis of the set of local and non-signaling conditional probabilities having a *fixed set of marginals*. We study this problem in a much more general setting than that of non-local games, by considering a bijection with combinatorial objects known as the *correlation polytope* and its relaxation. The correlation polytope is motivated by 0-1 programming and combinatorial optimization, and it is defined via its extremal points. To an arbitrary graph $G = (V, E)$ we associate a polytope $\text{COR}(G)$ in $\mathbb{R}^{|V|+|E|}$ defined by its extremal points $u = v \sqcup w$, where v is an arbitrary bit string of length $|V|$, while w is a bit string indexed by the edges $e = (x, y) \in E$ with $w_e = v_x \cdot v_y$. Pitowsky [Pit86] realized that there is an intimate connection between correlation polytopes associated to some graphs and the conditional probabilities that corresponds to classical strategies various non-local games. Moreover, it turns out that these questions are also instances of *classical marginal problems*, where one asks whether a given family of probability distributions is compatible, that is whether there exist a joint probability having the elements of the family as marginals. The connection between the local vs. non-signaling polytope in quantum information theory and the classical marginal problem is one of the main *conceptual contributions* of this work. These three equivalent formulations admit corresponding *relaxations*, i.e. larger polytopes with a simpler structure. We summarize this situation in the first two columns of the following table.

| Polytope | Relaxation | Slice |
|--------------------------|--------------------------|-----------------------------------|
| Classical strategies | Non-signaling strategies | <i>fixed Alice/Bob marginals</i> |
| Correlation polytope | LP-relaxation | <i>fixed vertex probabilities</i> |
| Compatible probabilities | All probabilities | <i>fixed 1-site marginals</i> |

In this paper, we shall study the *volume ratio* of *slices* of these polytopes. In the non-local game strategy point of view, the slices that we consider correspond to having fixed marginals $\mathbb{P}(a|x)$ and $\mathbb{P}(b|y)$. The corresponding notion of slice for the other equivalent formulations are summarized in

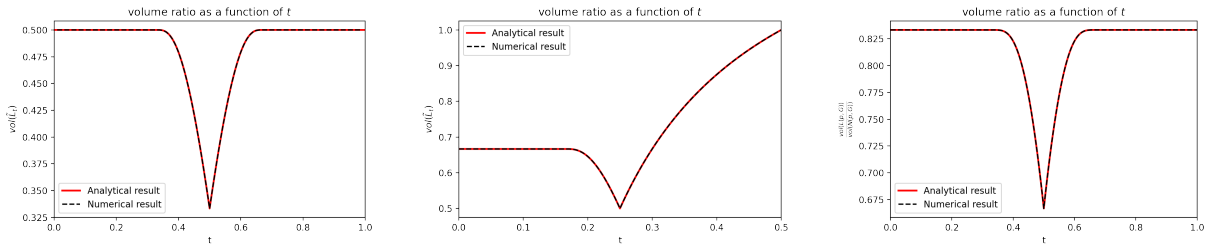
the third column of the table above. It is worth mentioning the formulation in terms of compatible probability distributions. We are given a graph $G = (V, E)$ and, and, for each vertex $v \in V$, some probability $p_v \in [0, 1]$. The volume ratio discussed above corresponds to the following probability:

For each edge $e = (v, w) \in E$, sample uniformly a joint probability distribution $(X_v^{(e)}, X_w^{(e)})$ such that $\mathbb{P}(X_v^{(e)} = 1) = p_v$ and $\mathbb{P}(X_w^{(e)} = 1) = p_w$. What is the probability that these pairwise distributions are compatible, i.e. that there exists a family $(Y_v)_{v \in V}$ such that

$$\forall (v, w) \in E, \quad (Y_v, Y_w) \stackrel{\text{dist}}{=} (X_v^{(e)}, X_w^{(e)})?$$

Similar volume ratio computations have been performed in the optimization literature, where the local and the non-signaling polytopes are known (at least in the case of complete graphs) as the *boolean quadric polytope* and its relaxation [Pad89]. In particular, the ratio of volumes has been proposed as a measure of the quality of approximation of the local polytope by the (simpler) non-signaling polytope [KLS97, LS20]. In the quantum information theory literature, the relative volumes of the classical and the non-signaling polytopes have been computed, in the CHSH game scenario, in [Cab05].

The *technical contribution* of this work is twofold. On the one hand, we compute the volume ratio of slices the local and the non-signaling polytopes associated of very simple graphs: the triangle, the square, and cyclic graphs in general, for different value of the parameters defining the slices. Note that the triangle graph corresponds to the *Bell-Wigner scenario* [Pit89c], the square graph corresponds to the *CHSH game* [CHSH69], while the cyclic graph on 5 vertices corresponds to the *KCBS scenario* [KCBS08]. Below are the plots corresponding to the triangle graph (with symmetric and non-symmetric slice parameters) and the square graph. The slice parameter t corresponds to Alice's and Bob's marginals being fixed Bernoulli distributions with parameter t . We refer to Propositions 6.2, 6.3 and 7.1 for the exact formulas.



The shape of the first and of the third graphs above (corresponding to slices having the same parameter) lead us to the second main technical contribution of this paper. One notices on this example that the volume ratio stays constant for values of the parameter t that are close to 0 or close to 1. We define the *fall-off* value $\tau(G)$ of the graph G to be the largest value of t for which the volume ratio is constant on the interval $[0, t]$. In the picture above, we have that the fall-off value of the triangle graph and that of the square graph in the symmetric cases (first and last graph) are equal to $\tau = 1/3$. This leads us to the second contribution of our work, which is more conceptual.

We study the value of the fall-off parameter for general graphs, and we conjecture that its inverse is one plus the *treewidth* of the graph. The conjecture is trivial for trees, and we prove it for graphs of treewidth two, i.e. *series-parallel* graphs. The conjecture is also supported by the values computed for simple graphs, such K_4 or K_5 (see Section 11 for tables containing these values for graphs with 4 and 5 vertices). Moreover, we study how the volume ratio and the fall-off value behave under simple graph operations, using Fourier-Motzkin elimination.

The paper is structured as follows. We start in Section 2 by introducing the topic from the marginal problem perspective. The next two sections contain a presentation of the equivalent

formulations: Section 3 from the perspective of correlation polytopes, while Section 4 from the perspective of quantum information theory. In Section 5 we precisely define the volume ratio as the probability that random bivariate distributions are compatible. Sections 6 to 9 contain the results about, respectively, the triangle graph (or the Bell-Wigner scenario), the square graph (or $K_{2,2}$, or the CHSH scenario), arbitrary cycle graphs, and the complete graph on four vertices K_4 . In Section 10 we gather several important results about general graphs, in particular our results about the relation between the fall-off value of the volume ratio and the treewidth of the graph. In the final Section 11 we summarize our work and present some open problems and future research directions.

2. THE CLASSICAL MARGINAL PROBLEM

The classical marginal problem can be informally stated as follows:

When can a set of probability distributions

$$\{p_J(x_{j_1}, \dots, x_{j_{|J|}})\}_{J \in \mathcal{J}}$$

be extended to a joint probability distribution of all the variables (x_i) ?

This is well-studied question in probability theory and statistics which goes back at least to Hoeffding [Hoe40] and Fréchet [Fré51]. One can formalize it as follows.

Definition 2.1. *Let $G = (V, E)$ be a (finite) hypergraph, where each vertex $v \in V$ comes with a finite alphabet \mathcal{X}_v . Each hyperedge $E \ni e \subsetneq V$ comes with a probability distribution p_e over the finite set*

$$X_e := \times_{v \in e} \mathcal{X}_v.$$

The classical marginal problem associated with the hypergraph G and the probability distributions $\{p_e\}_{e \in E}$ asks whether there exists a joint probability distribution p over the alphabet $\times_{v \in V} \mathcal{X}_v$ having all the p_e 's as marginals:

$$\forall e \in E, \forall x \in \mathcal{X}_e \quad p_e(x) = \sum_{y \in \mathcal{X}_{\bar{e}}} p(x, y),$$

where the variables in y correspond to vertices that do not belong to the hyperedge e . If such a p exist, we call the probabilities $(p_e)_{e \in E}$ G -compatible.

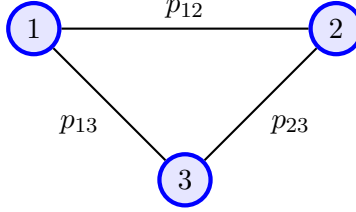
An obvious necessary condition for the marginal distributions to be G -compatible is that they should agree on their intersection:

$$\forall e, f \in E, \forall x \in \mathcal{X}_{e \cap f}, \quad \sum_{y \in \mathcal{X}_{e \setminus f}} p_e(x, y) = \sum_{z \in \mathcal{X}_{f \setminus e}} p_f(x, z). \quad (1)$$

Importantly, these conditions are not sufficient in the general case, making the classical marginal problem an interesting one. In order to give an example to this point, let us introduce the specialization of the classical marginal problem that we will deal with in the current work. We shall consider the following special case, consisting of two main points:

- The individual random variables will be *binary*, i.e. $\mathcal{X}_v = \{0, 1\}$, for all $v \in V$
- All the given marginals will be *bivariate*, i.e. $|e| = 2$, for all $e \in E$. In other words, $G = (V, E)$ will be a (simple, undirected) graph.

To illustrate the type of questions that we shall discuss in this work, consider the following triangle graph



where the three edge bivariate probabilities are identical:

$$p_{12}(\cdot, \cdot) = p_{13}(\cdot, \cdot) = p_{23}(\cdot, \cdot) = \begin{array}{|c|c|} \hline 0 & 1/2 \\ \hline 1/2 & 0 \\ \hline \end{array}$$

meaning that all three probabilities are given by

$$p_{ij}(a, b) = \begin{cases} 1/2 & \text{if } a \neq b \\ 0 & \text{if } a = b, \end{cases}$$

for $a, b \in \{0, 1\}$. These edge marginals clearly satisfy the condition from Eq. (1), since their marginals are all symmetric Bernoulli distributions $\mathbf{b}(1/2)$:

$$p_i(a) = \frac{1}{2} \quad a = 1, 2.$$

Note however that this particular classical marginal problem does not have a solution, that is the three marginals p_{12}, p_{13}, p_{23} are not K_3 -compatible. Indeed, if they were, there would exist binary random variables $X_{1,2,3}$ on a common probability space having the property

$$\mathbb{P}(X_1 \neq X_2) = \mathbb{P}(X_1 \neq X_3) = \mathbb{P}(X_2 \neq X_3) = 1,$$

which clearly is impossible since $X_i \in \{0, 1\}$. This is a toy example of the phenomenon of *frustration*, which has received a lot of attention in statistical physics.

3. SLICES OF THE CORRELATION POLYTOPE

As stated in the previous section, we shall focus in this work on the special case of the classical marginal problem where the given marginals are 2-partite. In this section we further specialize the problem, by fixing the single-variable marginals. This procedure can be very naturally formulated in terms of *correlation polytopes*, and slices thereof. They were introduced by Pitowsky in [Pit86] and have received a lot of attention in the recent years, see [DL94a, DL94b] and the references therein. In this section, we follow the presentation from [Pit91], adapted to the setting of this work. We first introduce the correlation polytope associated to a graph.

Definition 3.1. *Given a graph $G = (V, E)$, we define its correlation polytope*

$$\text{COR}(G) := \text{conv} \left\{ u_f ; f : V \rightarrow \{0, 1\} \right\} \subset \mathbb{R}^{|V|+|E|},$$

where u_f is the 0/1 vector having coordinates

$$\begin{aligned} \forall i \in V & \quad u_f(i) = f(i) \\ \forall e = (i, j) \in E & \quad u_f(e) = f(i)f(j). \end{aligned}$$

As an example, for the triangle graph K_3 discussed previously, the $2^3 = 8$ vectors u_f defined above are the rows of Table 1.

The correlation polytope is related to basic probability theory by the following crucial result.

| V-part | | | E-part | | |
|--------|---|---|--------|----|----|
| 1 | 2 | 3 | 12 | 13 | 23 |
| 0 | 0 | 0 | 0 | 0 | 0 |
| 0 | 0 | 1 | 0 | 0 | 0 |
| 0 | 1 | 0 | 0 | 0 | 0 |
| 0 | 1 | 1 | 0 | 0 | 1 |
| 1 | 0 | 0 | 0 | 0 | 0 |
| 1 | 0 | 1 | 0 | 1 | 0 |
| 1 | 1 | 0 | 1 | 0 | 0 |
| 1 | 1 | 1 | 1 | 1 | 1 |

TABLE 1. The extremal points of the correlation polytope corresponding to the triangle graph K_3 . The 8 extremal points have coordinates corresponding to the vertices of the graph (“the V-part”) and to the edges of the graph (“the E-part”). An entry e_{ij} of the E-part is computed using the AND operation of the vertices v_i and v_j .

Proposition 3.2 ([Pit91, Theorem 1.1]). *A vector p belongs to the correlation polytope $\text{COR}(G)$ if and only if there exist probability events $(A_i)_{i \in V}$ on some common probability space such that*

$$\begin{aligned} \forall i \in V, \quad p(i) &= \mathbb{P}(A_i) \\ \forall e = (i, j) \in E, \quad p(e) &= \mathbb{P}(A_i \cap A_j). \end{aligned}$$

The connection to the classical marginal problem from Definition 2.1 is now clear, by considering the distribution of the indicator random variables $X_v = \mathbb{1}_{A_v}$.

The correlation polytope is introduced via its V -representation, by a convex hull construction, giving an overcomplete list of vertices as the vectors u_f in Definition 3.1. We refer the reader to [Zie12] for the background on the convex geometry of polytopes. We recall here that a polytope has two mathematically equivalent representations:

- the V -representation, as a convex hull of its (finitely many) extremal points
- the H -representation, as an intersection of (finitely many) half-spaces defined by its facets.

Obtaining a concise list of facet-defining inequalities (i.e. the H -representation) for correlation polytopes is an active field of current research; partial results are known for small graphs of interest, while the general question of testing membership in $\text{COR}(G)$ is NP-complete in general [Pit91, Section 3]. The complete set of inequalities (the H -representation) for the triangle graph K_3 consists of 16 inequalities and is given explicitly in Eqs. (11) and (12).

We now come to the main object of study of this paper, particular slices of the correlation polytope, obtained by fixing the uni-variate probabilities $\{p_i\}_{i \in V}$.

Definition 3.3. *Given a graph $G = (V, E)$ and a vector of probabilities $p \in [0, 1]^{|V|}$, we define the correlation slice*

$$\text{COR}(p, G) := \{u \in \text{COR}(G) : \forall i \in V, u(i) = p(i)\} \subset \mathbb{R}^{|E|}.$$

Clearly, $\text{COR}(p, G)$ is a non-empty polytope, since it contains the point

$$\left(p(i)p(j) \right)_{(i,j) \in E}$$

corresponding to independent events A_i in Proposition 3.2.

For every edge $e = (i, j) \in E$, the value $p_e \equiv p_{ij}$ completely determines the bivariate probability in the setting of the classical marginal problem:

$$\begin{array}{ccc}
\sum = 1 - p_j & \sum = p_j & \\
\uparrow & \uparrow & \\
0 & 1 & \\
\sum = 1 - p_i \leftarrow 0 & \begin{array}{|c|c|} \hline 1 - p_i - p_j + p_{ij} & p_j - p_{ij} \\ \hline p_i - p_{ij} & p_{ij} \\ \hline \end{array} & \\
\sum = p_i \leftarrow 1 & &
\end{array}$$

Hence, in order for the vector $(p_{ij})_{(i,j) \in E}$ to be an element of the correlation slice, the following four elements need to be positive:

$$\begin{aligned}
1 - p_i - p_j + p_{ij} &\geq 0 \\
p_i - p_{ij} &\geq 0 \\
p_j - p_{ij} &\geq 0 \\
p_{ij} &\geq 0.
\end{aligned} \tag{2}$$

These conditions state precisely the fact that the bivariate probability distribution above belongs to the transportation polytope defined by the Bernoulli distributions $\mathbf{b}(p_i)$ and $\mathbf{b}(p_j)$. We are thus led to introduce the following polytope.

Definition 3.4. *Given a graph $G = (V, E)$ and a vector of probabilities $p \in [0, 1]^{|V|}$, we define the transportation slice*

$$\text{TRA}(p, G) := \prod_{e=(i,j) \in E} \left[\max(0, p_i + p_j - 1), \min(p_i, p_j) \right].$$

The transportation slice is a cartesian product of slices of transportation polytopes, and encodes the trivial, uncoupled, inequalities that the bivariate probabilities p_{ij} need to satisfy in order to belong to the correlation slice. For example, in our running example of the triangle graph K_3 , these are the inequalities (11) (at fixed p_i, p_j). We have the following obvious result.

Proposition 3.5. *For all graphs $G = (V, E)$, and for all vectors $p \in [0, 1]^{|V|}$,*

$$\text{COR}(p, G) \subseteq \text{TRA}(p, G). \tag{3}$$

Actually, in order to mimic the construction of the correlation slice from Definition 3.3, one can construct a transportation body associated to a graph G , such that the transportation slice can be obtained by fixing the V -coordinates of the transportation body. Note that we choose to call this polytope the transportation body in order to avoid any confusion with the established terminology of transportation polytope.

Definition 3.6. *Given a graph $G = (V, E)$, we define the transportation body*

$$\text{TRA}(G) := \{(p, q) \in [0, 1]^{|V|} \times [0, 1]^{|E|} : q \in \text{TRA}(p, G)\}.$$

Similarly to Proposition 3.5, we have the following inclusion:

$$\text{COR}(G) \subseteq \text{TRA}(G).$$

The goal of the rest of the paper is to study the inclusion in Eq. (3) and to quantify how close it is to being an equality. It is a well-know fact that for trees, we have an equality.

Proposition 3.7. [BM10, Theorem V.2] *If $G = (V, E)$ is a tree, then*

$$\text{COR}(G) = \text{TRA}(G).$$

Equivalently, for all vectors $p \in [0, 1]^{|V|}$ we have

$$\text{COR}(p, G) = \text{TRA}(p, G).$$

Proof. For a tree G with vertex degrees $d(v)$, one can show that the following joint probability distribution has the correct 2-marginals

$$p(x_1, x_2, \dots, x_{|V|}) := \frac{\prod_{e=(v,w) \in E} p_e(x_v, x_w)}{\prod_{v \in V} p_v(x_v)^{d(v)-1}},$$

by recursively eliminating the leaves of the tree; see Definition 2.1. \square

The reciprocal implication is also true.

Proposition 3.8 ([Pad89, Proposition 8]). *The correlation and the transportation bodies are equal $\text{COR}(G) = \text{TRA}(G)$ iff G is a forest, i.e. a collection of trees.*

4. RELATION TO QUANTUM INFORMATION THEORY AND CONTEXTUALITY

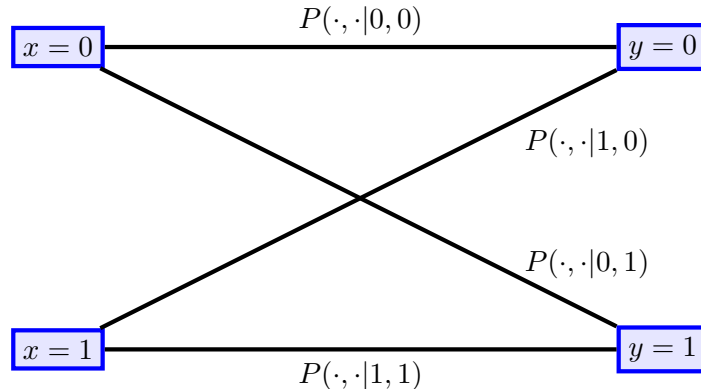
In this section we would like to shed light on the connection between the transportation body and correlation polytope and the no-signaling and local polytopes obtained in non-local games in quantum information theory. This connection was the main motivation for our work, and the main objects we shall investigate in the rest of the paper are inspired by quantum information theory.

Let us first describe the setting of *non-local games* from quantum information theory [PV16]. These mathematical scenarios are modern formulations of (thought [Bel64]) experiments [AGR82, HBD⁺15] in foundational quantum mechanics related to non-locality. We consider below the case of the complete bipartite graph $G = K_{2,2}$ which is connected to the CHSH game [CHSH69] in quantum information theory. Let us first discuss how the the polytopes $\text{COR}(K_{2,2})$ and $\text{TRA}(K_{2,2})$ are related to the correlations $P(ab|xy)$ corresponding to the CHSH game. In that game, two players, Alice and Bob, receive binary questions $x, y \in \{0, 1\}$ and provide binary answers $a, b \in \{0, 1\}$. In the CHSH game, the players win if their answers satisfy $a \oplus b = x \cdot y$, but this rule is irrelevant to us; we focus here only on possible 4-tuples x, y, a, b and their probability distribution. Alice and Bob cannot communicate during the game, hence the conditional probabilities they generate must obey the *non-signaling relations*: the marginal over Bob's answer b of P cannot depend on Bob's question y , and vice-versa

$$\forall a, x, \quad \sum_{b=0,1} P(a, b|x, 0) = \sum_{b=0,1} P(a, b|x, 1) \quad (4)$$

$$\forall b, y, \quad \sum_{a=0,1} P(a, b|0, y) = \sum_{a=0,1} P(a, b|1, y). \quad (5)$$

This means that the four bivariate probability distributions $P(\cdot, \cdot|x, y)$, for $x, y \in \{0, 1\}$ have compatible marginals as described above, so one can attach them to the edges of the bipartite graph $K_{2,2}$, as below:



Hence, to a conditional probability P satisfying the non-signaling equations (4)-(5), we associate the following element of the polytope $\text{TRA}(K_{2,2})$:

$$\left[\overbrace{P(a=1|0, \cdot), P(a=1|1, \cdot), P(b=1|\cdot, 0), P(b=1|\cdot, 1)}^{\text{vertices}}, \right. \\ \left. \underbrace{P(1, 1|0, 0), P(1, 1|0, 1), P(1, 1|1, 0), P(1, 1|1, 1)}_{\text{edges}} \right] \in \mathbb{R}^{4+4}. \quad (6)$$

Importantly, from the data above, using the non-signaling equations, one can recover the whole probability distribution P . Given now some fixed set of marginals

$$\begin{aligned} p_0^A &= P(a=1|x=0, y=\cdot) \\ p_1^A &= P(a=1|x=1, y=\cdot) \\ p_0^B &= P(b=1|x=\cdot, y=0) \\ p_1^B &= P(b=1|x=\cdot, y=1), \end{aligned}$$

one can consider the slice $\text{TRA}((p_0^A, p_1^A, p_0^B, p_1^B), K_{2,2})$, consisting of 4-tuples

$$\left(P(1, 1|0, 0), P(1, 1|0, 1), P(1, 1|1, 0), P(1, 1|1, 1) \right).$$

From this information, one can recover the whole set of joint game probabilities P having fixed vertex-marginals $(p_0^A, p_1^A, p_0^B, p_1^B)$. This type of slice will be the main focus of our work.

Having related the (slices of the) transportation polytope $\text{TRA}(K_{2,2})$ to conditional probabilities appearing in the CHSH game and satisfying the non-signaling conditions (i.e. $\mathbf{N}(K_{2,2})$), let us now describe the correlation polytope $\text{COR}(K_{2,2})$ in terms of the local probabilities P appearing in the CHSH game. To this end, recall that a game strategy P is called *local* if there exists a *hidden variable* λ with probability distribution Q , and local probabilities P_A, P_B such that

$$P(a, b|x, y) = \sum_{\lambda} Q(\lambda) P_A(a|x, \lambda) P_B(b|y, \lambda).$$

The convex set of local probabilities P is the convex hull of its extremal points, the set of *deterministic* strategies, where Q is a delta function, and, for each pair (player, question) (i.e. for each vertex of the graph $K_{2,2}$), there is a deterministic answer, 0 or 1. This choice is encoded precisely in the function f from Definition 3.1, while the corresponding vector Eq. (6) is given by u_f . This shows how the correlation polytope $\text{COR}(K_{2,2})$ is related to the local polytope $\mathbf{L}(K_{2,2})$. One can rephrase this using *Fine's theorem* [Fin82]: a conditional probability P is local iff it can be written as a convex mixture of local deterministic processes:

$$P(ab|xy) = \sum_{j,k} r_{j,k} \mathbb{1}_{a=j(x)} \mathbb{1}_{b=k(y)} \quad (7)$$

Finally, let us point out that non-local games where Alice and Bob receive m , respectively n questions, and must provide binary answers, can be easily reformulated in terms of the transportation body and correlation polytope for the *bipartite complete graph* $K_{m,n}$.

Let us now put forward the connection between the transportation body and correlation polytope *contextuality theory*. In the Bell scenario, we are only concerned with correlations of outcomes of measurements which are spatially separated, hence the notion of locality and no-signaling. Contextuality is the generalization of Bell scenarios to include correlations among all compatible observables. The set of these compatible observables forms a *context*. Hence, for a set of observables $X = \{X_0, X_1, \dots, X_n\}$, a subset $c \subseteq X$ forms a context if $\forall i, j : X_i, X_j \in c, X_i$ is compatible with X_j .

Following [CF12] (we refer the reader to [Sca19] for a detailed description of Bell scenarios), we start with a hidden-variable λ which completely defines the process of obtaining outcomes corresponding to any observable X_i . Thus, the probabilities $\rho(\lambda)$ associated with different processes must follow $\rho(\lambda) \geq 0$ and $\sum_{\lambda} \rho(\lambda) = 1$. Completeness implies that the distribution $P(x_i|X_i\lambda)$ is independent of all other observables.

Clearly, for two compatible observables X_i and X_j , we have,

$$P(x_i x_j | X_i X_j) = \sum_{\lambda} \rho(\lambda) P(x_i | X_i) P(x_j | X_j) \quad (8)$$

This is equivalent to saying that the observables are non-contextual (compatible) iff it can be written as a convex mixture of deterministic processes. [Fin82]

$$P(x_i x_j | X_i X_j) = \sum_{k,l} r_{k,l} \mathbb{1}_{x_i=k(X_i)} \mathbb{1}_{x_j=l(X_j)} \quad (9)$$

where, $r_{j,k} \geq 0$ and $\sum_{j,k} r_{j,k} = 1$. This is true in general for any number of compatible observables. We will only be studying cases with cardinality of contexts less than or equal to 2.

Notice that each row in the truth table for the non-contextual polytope denotes one of these deterministic processes and the convex sum of the rows yields any point in the correlation polytope. Hence, the correlation polytope and the non-contextual polytope have the same mathematical structure.

Now, consider dichotomic outputs $\{0,1\}$ for all observables and define $P(1|X_1)$ as p_{a_1} and $P(1|X_2)$ as p_{b_1} where X_1 and X_2 form a context. Clearly, $p_{a_0} = 1 - p_{a_1}$ and $p_{b_0} = 1 - p_{b_1}$. Notice that these probabilities exactly mimic the behaviour described by inequalities Eq. (2) and hence, the no-disturbance body has the same structure as that of the transportation body. This establishes the connection between the objects studied in this paper and contextuality. Finally, let us point out that there exists another theoretical framework for contextuality, based on (hyper-)graphs [CSW14, AFLS15], where vertices correspond to outcomes and hyperedges to measurements. It is argued in [AFLS15, Appendix D] that the observable based approach and the hypergraph based approach are equivalent. Note that in both the setting of the current paper and in [AFLS15] (the probabilistic model), to each vertex of a graph one associates a number $p(v) \in [0, 1]$. The meaning of this assignment is completely different: in our setting, there are no other vertices v_2, \dots, v_k such that the sum $p(v) + p(v_2) + \dots + p(v_k) = 1$, whereas in [AFLS15, Definition 2.4.1] these vertices appear explicitly in the graph.

From now on, for the sake of brevity, and in order to emphasize further the connection with quantum information theory, we shall use the notation \mathbf{L} (resp. \mathbf{N}) to denote the correlation polytope \mathbf{COR} (resp. the transportation polytope \mathbf{TRA}) and their slices:

$$\begin{aligned} \mathbf{L}(G) &:= \mathbf{COR}(G) \\ \mathbf{N}(G) &:= \mathbf{TRA}(G) \\ \mathbf{L}(p, G) &:= \mathbf{COR}(p, G) \\ \mathbf{N}(p, G) &:= \mathbf{TRA}(p, G), \end{aligned}$$

where $G = (V, E)$ is any graph and p is a vector of probabilities $p \in [0, 1]^{|V|}$.

To conclude, we have shown in this section that the marginal problem we introduced in Section 2, in the case of the square graph $C_4 = K_{2,2}$, is intimately related to the CHSH non-local game, with the constraint of fixed marginals for Alice and Bob. This situation can be naturally generalized to all bipartite complete graphs $K_{m,n}$, which correspond to non-local games with two answers per player and m , respectively n , questions. The volume ratio question for the $K_{2,2}$ graph will be discussed at length in Section 7. Other graphs, such as the triangle graph, cyclic graphs, or the K_4 graph, are discussed in Sections 6, 8 and 9.

5. RANDOM MARGINAL PROBLEMS

Motivated by questions in quantum information theory, we have introduced in the previous sections, for a given graph $G = (V, E)$ and a given vector of probabilities $p \in [0, 1]^{|V|}$, the *local slice* (the correlation slice), resp. the *non-signaling slice* (the transportation slice)

$$\mathbf{L}(p, G) \subseteq \mathbf{N}(p, G) \subset \mathbb{R}^{|E|}.$$

Given its cartesian product structure, the set $\mathbf{N}(p, G)$ comes equipped with a natural probability measure that is easy to compute with, the normalized Lebesgue measure:

$$\eta(p, G) := \bigotimes_{(i,j) \in E} \frac{\mathbb{1}_{[\max(0, p_i + p_j - 1), \min(p_i, p_j)]}}{\min(p_i, p_j) - \max(0, p_i + p_j - 1)} dx \quad (10)$$

The probability measure η defined above is precisely the uniform (normalized) volume measure on the (scaled) hypercube introduced in Definition 3.4.

In what follows, we shall provide a partial answer to the following fundamental question:

$$\mathbb{P}_{q \sim \eta(p, G)} \left[q = (q_{ij})_{(i,j) \in E} \in \mathbf{L}(p, G) \right] = ?$$

Equivalently, this quantity can be also understood as the volume ratio

$$\frac{\text{vol}(\mathbf{L}(p, G))}{\text{vol}(\mathbf{N}(p, G))}$$

between corresponding slices of the local and the non-signaling polytopes. As mentioned in the introduction, a similar question for the non-sliced bodies has been studied in the context of (approximating) the boolean quadric polytope [Pad89, KLS97, LS20].

To quantify the properties of the volume ratio for sliced bodies, we define the following parameters:

Definition 5.1. *For a given graph $G(V, E)$ and symmetric marginals $p_i = t \forall i \in V$, we define the fall-off value $\tau(G)$ as the value of t after which the volume ratio $\text{vol}(\mathbf{L}(G)_t) / \text{vol}(\mathbf{N}(G)_t)$ is no longer constant:*

$$\tau(G) := \sup \left\{ t : \frac{\text{vol}(\mathbf{L}(G)_t)}{\text{vol}(\mathbf{N}(G)_t)} \text{ is constant on } (0, t) \right\} \in [0, 1/2].$$

Above, we write

$$\mathbf{S}(G)_t := \mathbf{S}(p = (t, t, \dots, t), G) \quad \text{for a set } \mathbf{S} = \mathbf{L}, \mathbf{N}.$$

For trees T , we have seen in Proposition 3.7 that $\tau(T) = 1/2$

Proposition 5.2. *For any graph G , $\tau(G) > 0$. In other words, the volume ratio $\text{vol}(\mathbf{L}(G)_t) / \text{vol}(\mathbf{N}(G)_t)$ is constant on some non-empty interval $t \in (0, \tau)$.*

Proof. This follows since we have finitely many inequalities that can cut at some $t > 0$, so the polytopes $\mathbf{L}(G)_t$ and $\mathbf{N}(G)_t$ are equal up to some time τ . \square

We introduce next two important values of the volume ratio: the one of the constant portion $t \in (0, \tau)$ and the one in the middle, $t = 1/2$.

Definition 5.3. *For a given graph $G(V, E)$ and associated marginals $p_i = t \forall i \in V$, we define the initial ratio $\rho_{0+}(G)$, as the volume ratio for all values $t \in (0, \tau(G))$; in particular*

$$\rho_{0+}(G) := \frac{\text{vol}(\mathbf{L}(G)_{\tau/2})}{\text{vol}(\mathbf{N}(G)_{\tau/2})}.$$

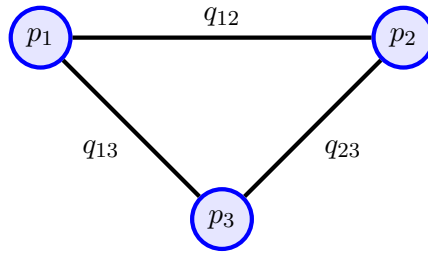
We also define middle ratio $\rho_{1/2}(G)$ as the volume ratio at $t = 1/2$:

$$\rho_{1/2}(G) := \frac{\text{vol}(\mathbf{L}(G)_{1/2})}{\text{vol}(\mathbf{N}(G)_{1/2})}.$$

6. THE TRIANGLE GRAPH

Having set the stage, it is instructional that we consider specific examples. We start by looking at the complete graph with three vertices, K_3 . This is also the smallest non-trivial graph which is not a tree (recall that for trees, $\mathbf{L} = \mathbf{N}$, see Proposition 3.7).

The K_3 graph corresponds to the Bell-Wigner Polytope [Pit89a], [Pit89b]. The physical scenario in question is measurements performed on a bipartite state (such as the singlet state) with each component of the state being measured in one of three distinct directions (3 questions) with binary outputs (2 answers for each question) [Wig97].



The V -representation of $\mathbf{L}(K_3) = \text{COR}(K_3)$ for this graph has already been given in Table 1. The corresponding H -representation reads:

$$\begin{aligned} 0 \leq q_{ij} \leq \min(p_i, p_j) \\ p_i + p_j - q_{ij} \leq 1 \end{aligned} \tag{11}$$

$$\begin{aligned} p_1 + p_2 + p_3 - q_{12} - q_{13} - q_{23} \leq 1 \\ -p_1 + q_{12} + q_{13} - q_{23} \leq 0 \\ -p_2 + q_{12} - q_{13} + q_{23} \leq 0 \\ -p_3 - q_{12} + q_{13} + q_{23} \leq 0 \end{aligned} \tag{12}$$

Note that we have in this case 6 variables: 3 corresponding to the vertices of K_3 (p_1, p_2, p_3) and 3 corresponding to the edges (q_{12}, q_{13}, q_{23}). Hence, polytopes of interest have 6 coordinates:

$$\mathbf{L}(K_3) = \text{COR}(K_3) \subseteq \mathbf{N}(K_3) = \text{TRA}(K_3) \subset \mathbb{R}^6.$$

Inequalities in Eq. (11) are precisely those appearing in Definition 3.3 and thus define the set $\mathbf{N}(K_3)$. The inequalities Eq. (12) are the additional constraints distinguishing $\mathbf{L}(K_3)$ from $\mathbf{N}(K_3)$. The volumes of these bodies have been computed respectively in [LS20, Theorems 16 and 19]:

$$\text{vol}(\mathbf{N}(K_3)) = \frac{1}{120} \quad \text{and} \quad \text{vol}(\mathbf{L}(K_3)) = \frac{1}{180} = \frac{2}{3} \text{vol}(\mathbf{N}(K_3)).$$

As stated in the introduction, the main philosophy of our work is to understand the inclusion $\mathbf{L}(K_3) \subseteq \mathbf{N}(K_3)$ via *slices* of these polytopes, and to see the slice inclusion problem as a classical marginal problem.

In this section we shall consider two such slices, studied separately in the following two subsections. The slices are obtained by fixing the values of the vertex parameters p and studying the 3-dimensional polytopes of the q variables.

6.1. **Symmetric slices** $(p_1, p_2, p_3) = (t, t, t)$. We first consider the most symmetric case, where all the vertex variables $p_{1,2,3}$ of the correlation polytope of the triangle graph are equal:

$$p_1 = p_2 = p_3 =: t \in [0, 1].$$

Plugging in these marginals, we obtain the H -representation defining our slice $\mathbf{L}(p = (t, t, t), K_3)$:

$$\max\{0, 2t - 1\} \leq q_{ij} \leq t \quad (13)$$

$$\begin{aligned} q_{12} + q_{13} + q_{23} &\geq 3t - 1 \\ q_{12} + q_{13} - q_{23} &\leq t \\ q_{12} - q_{13} + q_{23} &\leq t \\ -q_{12} + q_{13} + q_{23} &\leq t. \end{aligned} \quad (14)$$

As before, Eq. (13) corresponds to the no-signaling slice $\mathbf{N}(p = (t, t, t), K_3)$. In what follows, we shall denote the polytopes of interest by

$$\mathbf{N}_t := \mathbf{N}(p = (t, t, t), K_3) = \{(q_{12}, q_{13}, q_{23}) \in \mathbb{R}^3 : \text{Eq. (13) holds}\}$$

$$\mathbf{L}_t := \mathbf{L}(p = (t, t, t), K_3) = \{(q_{12}, q_{13}, q_{23}) \in \mathbb{R}^3 : \text{Eq. (13) and Eq. (14) hold}\}.$$

Since our measurements are dichotomic (with outcomes say, 0 and 1), the assignment of possible outcomes to the random variables is symmetric with respect to swapping the two possible outcomes (bit-flip). Hence, we have the following obvious symmetry.

Proposition 6.1. *The involution $(q_{12}, q_{13}, q_{23}) \mapsto (1 - q_{12}, 1 - q_{13}, 1 - q_{23})$ maps isometrically $\mathbf{N}_t \leftrightarrow \mathbf{N}_{1-t}$ and $\mathbf{L}_t \leftrightarrow \mathbf{L}_{1-t}$ for all $t \in [0, 1]$.*

Thus, we will keep our study limited to $t \in [0, 1/2]$. This ensures that Eq. (13) simplifies to $0 \leq q_{ij} \leq t$. Note that the case $t = 0$ (or, equivalently, $t = 1$), corresponding to the deterministic scenario, is degenerate:

$$\mathbf{N}_0 = \mathbf{L}_0 = \{(0, 0, 0)\}.$$

We shall thus assume from now on $t \in (0, 1/2]$.

Before we explicitly calculate the volumes of \mathbf{L}_t and \mathbf{N}_t , we will do one final simplification. Substituting $q_{ij} \rightarrow tx_{ij}$, the inequalities (13) and (14) become:

$$0 \leq x_{ij} \leq 1 \quad (15)$$

$$x_{12} + x_{13} + x_{23} \geq 3 - \frac{1}{t} \quad (16a)$$

$$x_{12} + x_{13} - x_{23} \leq 1 \quad (16b)$$

$$x_{12} - x_{13} + x_{23} \leq 1 \quad (16c)$$

$$-x_{12} + x_{13} + x_{23} \leq 1 \quad (16d)$$

We introduce the new, scaled, polytopes:

$$\tilde{\mathbf{N}}_t := \{(x_{12}, x_{13}, x_{23}) \in \mathbb{R}^3 : \text{Eq. (15) holds}\}$$

$$\tilde{\mathbf{L}}_t := \{(x_{12}, x_{13}, x_{23}) \in \mathbb{R}^3 : \text{Eq. (15) and Eq. (16) hold}\}.$$

Clearly, one has $\text{vol}(\mathbf{N}_t) = t^3 \text{vol}(\tilde{\mathbf{N}}_t)$, and similarly for the local polytope; hence

$$\frac{\text{vol}(\mathbf{L}_t)}{\text{vol}(\mathbf{N}_t)} = \frac{\text{vol}(\tilde{\mathbf{L}}_t)}{\text{vol}(\tilde{\mathbf{N}}_t)}.$$

From inequality (15), it becomes easy to see that $\tilde{\mathbf{N}}_t$ is the unit cube $[0, 1]^3$ and thus $\text{vol}(\tilde{\mathbf{N}}_t) = 1$, independently of the value of t .

The computation for the scaled local polytope slice \tilde{L}_t is more involved. First, we note that Eq. (16a) depends on t , while Eqs. (16b) to (16d) are independent of t . Importantly, Eq. (16a) is trivially true for all $t \in (0, 1/3]$. Hence, the volume of the local slice is constant in this region.

We assume for now $t \leq 1/3$. In this regime, to explicitly compute the volume, we go to the V -representation of \tilde{L}_t . The polytope \tilde{L}_t has the following vertices

$$(0, 0, 0), (1, 0, 0), (0, 1, 0), (0, 0, 1), (1, 1, 1).$$

The corresponding 3-dimensional body is depicted in Figure 1. We partition it into two disjoint bodies:

- a triangular pyramid

$$\text{conv} \left\{ (0, 0, 0), (1, 0, 0), (0, 1, 0), (0, 0, 1) \right\}$$

which has volume $1/6$

- a regular tetrahedron

$$\text{conv} \left\{ (1, 1, 1), (1, 0, 0), (0, 1, 0), (0, 0, 1) \right\}$$

with side length $\sqrt{2}$ and volume $1/3$.

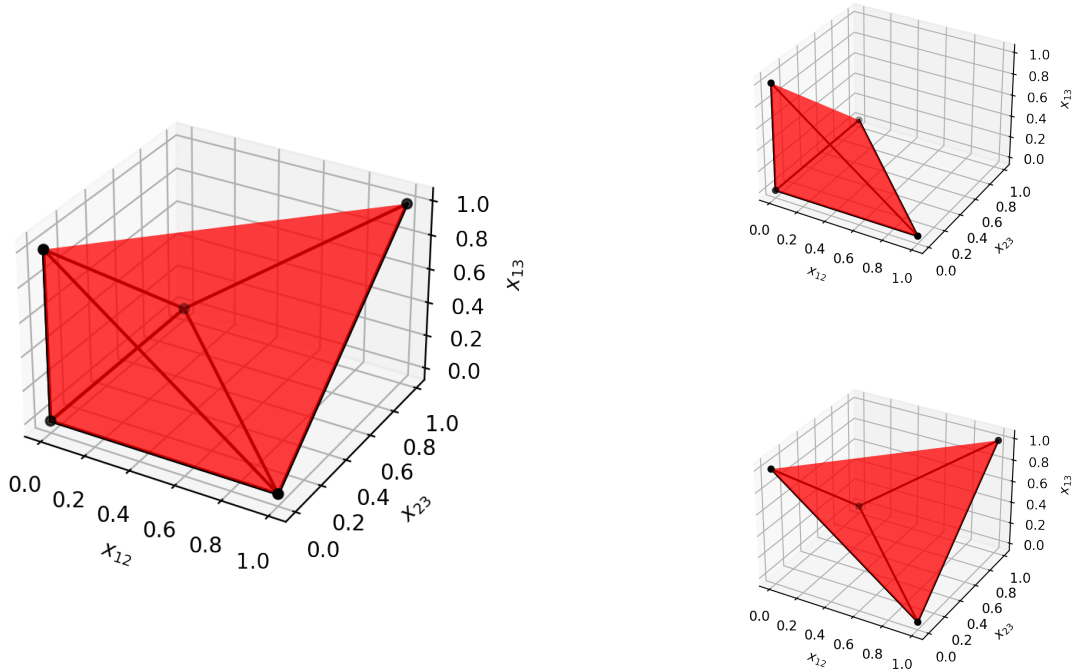


FIGURE 1. The scaled local polytope slice \tilde{L}_t , for $0 < t \leq 1/3$ (left). In the right panel, we partition it into a triangular pyramid and a regular tetrahedron.

Hence, the volume of the combined region is:

$$\forall t \in (0, 1/3] \quad \text{vol}(\tilde{L}_t) = \frac{1}{3} + \frac{1}{6} = \frac{1}{2}. \quad (17)$$

We now move on to the case $t \in (1/3, 1/2]$. The inequality (16a) is non-trivial, and the body $\tilde{\mathcal{L}}_t$ will depend on the actual value of the parameter t . The V -representation for $\tilde{\mathcal{L}}_t$ in this parameter region is

$$\text{conv} \left\{ (s, 0, 0), (0, s, 0), (0, 0, s), (0, 1, 0), (0, 0, 1), (1, 1, 1) \right\},$$

where $s := 3 - 1/t$. The 3-dimensional polytope spanned is shown in Fig. 2.

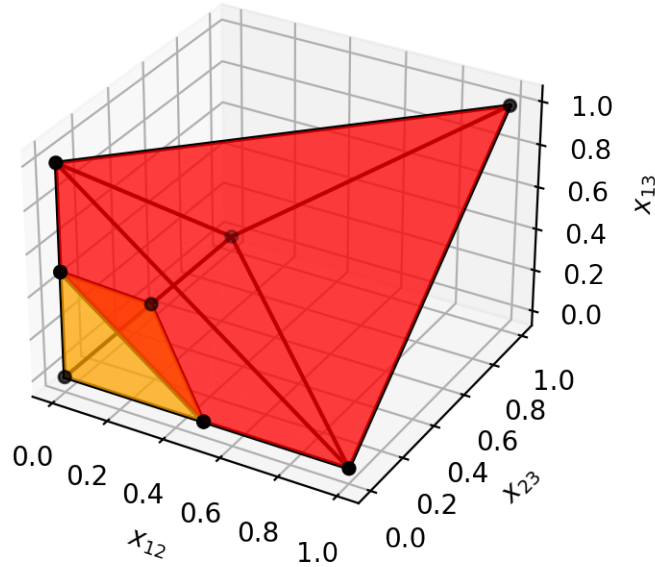


FIGURE 2. The scaled local polytope slice $\tilde{\mathcal{L}}_t$, for $1/3 < t \leq 1/2$ (in red). The yellow region represents the difference between this case and the case when $t \leq 1/3$, see Fig. 1.

The enclosed region has the same volume as the region in Fig. 1, left panel, minus the volume of region $\text{conv} \left\{ (s, 0, 0), (0, s, 0), (0, 0, s), (0, 0, 0) \right\}$ which is represented in yellow in Fig. 2. This again is just the region displayed in Fig. 1, top-right panel, scaled by s :

$$\text{vol}(\text{bottom-left, yellow region in Fig. 2}) = \frac{s^3}{6}.$$

Hence, we have:

$$\forall t \in (1/3, 1/2] \quad \text{vol}(\tilde{\mathcal{L}}_t) = \frac{1}{2} - \frac{s^3}{6} = \frac{1}{2} - \frac{(3 - 1/t)^3}{6}. \quad (18)$$

Putting everything together and using Proposition 6.1, we obtain the main result of this section.

Proposition 6.2. *The volume ratio of symmetric slices ($p_1 = p_2 = p_3 = t$) between the local and the non-signaling polytopes corresponding to the triangle graph K_3 is given by:*

$$\frac{\text{vol}(\mathbf{L}_t)}{\text{vol}(\mathbf{N}_t)} = \begin{cases} \frac{1}{2}, & t \in (0, \frac{1}{3}] \\ \frac{1}{2} - \frac{(3-1/t)^3}{6}, & t \in (\frac{1}{3}, \frac{1}{2}] \\ \frac{1}{2} - \frac{(3-1/(1-t))^3}{6}, & t \in (\frac{1}{2}, \frac{2}{3}] \\ \frac{1}{2}, & t \in (\frac{1}{3}, 1). \end{cases}$$

The various parameters as defined in Section 5 are:

$$\text{The fall-off value } \tau(K_3) = \frac{1}{3}$$

$$\text{The initial ratio } \rho_{0+}(K_3) = \frac{1}{2}$$

$$\text{The middle ratio } \rho_{1/2}(K_3) = \frac{1}{3}.$$

We plot the analytical results alongside numerical calculations using the `cddlib` library [Fuk23] in Fig. 3.

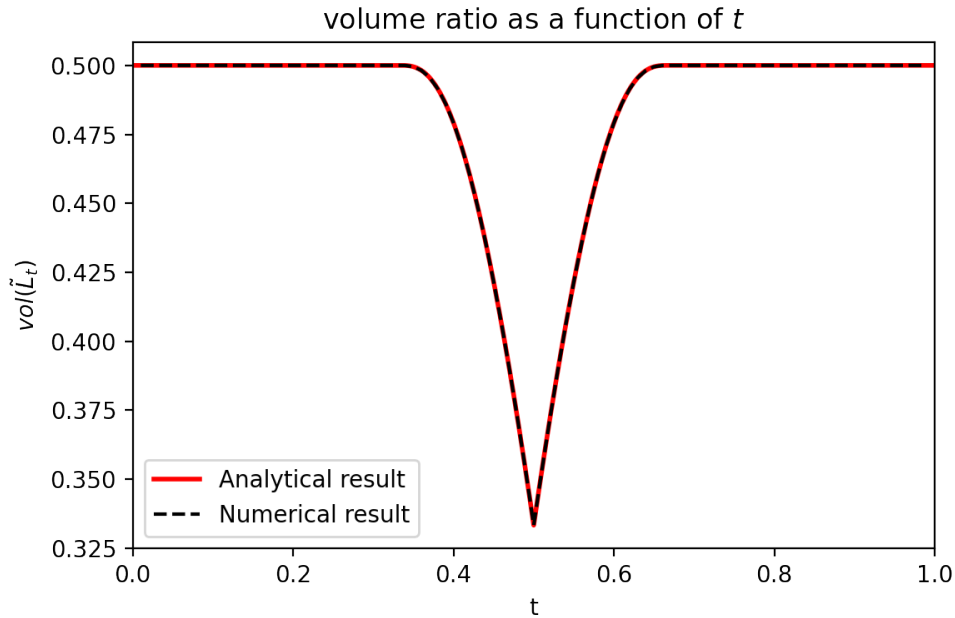


FIGURE 3. Volume ratio between the local polytope slice and the non-signaling polytope slice, in the symmetric ($p_i = t$) case. The curve is symmetric with respect to $t = 1/2$, and constant ($= 1/2$) for $t \leq 1/3$.

6.2. Skewed slices (p_1, p_2, p_3) = $(t, t, 1/2 - t)$. We now consider a different, non-symmetric, slice through the local and non-signaling polytopes of the triangle graph. For a parameter $t \in [0, 1/2]$, we consider the slice corresponding to the vertex probabilities

$$p_1 = p_2 = t, \quad p_3 = 1/2 - t.$$

Note that this is the only situation of this type that we shall consider in this paper. The previous subsection, as well as all of the subsequent examples will focus on symmetric slices, where all the probabilities associated to vertices are equal.

Using the same symmetry argument as in Proposition 6.1, this slice is isometrically equivalent to the one corresponding to

$$p_1 = p_2 = 1 - t, \quad p_3 = t - 1/2, \quad \text{for } t \in [1/2, 1].$$

As in the previous case, we denote by \mathbf{N}_t and \mathbf{L}_t the respective slices. The case $t = 0$ yields degenerate sets, so we assume that $t \in (0, 1/2]$.

Replacing this parameterization for the marginals in Eq. (11) and Eq. (12), we have the H -representation defining our slice \mathbf{L}_t as:

$$\begin{aligned} 0 &\leq q_{12} \leq t \\ 0 &\leq q_{13}, q_{23} \leq \min \left\{ t, \frac{1}{2} - t \right\} \end{aligned} \tag{19}$$

$$\begin{aligned} q_{12} + q_{13} + q_{23} &\geq t - \frac{1}{2} \\ q_{12} + q_{13} - q_{23} &\leq t \\ q_{12} - q_{13} + q_{23} &\leq t \\ -q_{12} + q_{13} + q_{23} &\leq \frac{1}{2} - t \end{aligned} \tag{20}$$

where inequalities (19) form the H -representations of \mathbf{N}_t and inequalities (20) are the additional inequalities constraining \mathbf{L}_t . Following a similar approach as in the symmetric case, we substitute $q_{ij} = tx_{ij}$, obtaining the inequalities for the scaled bodies $\tilde{\mathbf{N}}_t, \tilde{\mathbf{L}}_t$:

$$\begin{aligned} 0 &\leq x_{12} \leq 1 \\ 0 &\leq x_{13}, x_{23} \leq \min \left\{ 1, \frac{1}{2t} - 1 \right\} \end{aligned} \tag{21}$$

$$x_{12} + x_{13} + x_{23} \geq 1 - \frac{1}{2t} \tag{22a}$$

$$x_{12} + x_{13} - x_{23} \leq 1 \tag{22b}$$

$$x_{12} - x_{13} + x_{23} \leq 1 \tag{22c}$$

$$-x_{12} + x_{13} + x_{23} \leq \frac{1}{2t} - 1. \tag{22d}$$

Unlike the symmetric slice case discussed previously, the present situation is more involved since $\text{vol}(\tilde{\mathbf{N}}_t)$ is not equal to 1 in the entire domain here. We note that inequality (22a) is always satisfied for $t \in (0, 1/2)$ and hence it can be dropped. Inequalities (22b) and (22c) are independent of t , while (22d) is trivially satisfied in the range $t \in (0, 1/6]$.

Hence, we start by first looking at the region $t \in (0, 1/6]$. The H -representation of $\tilde{\mathbf{L}}_t$ is given by the relevant inequalities:

$$0 \leq x_{ij} \leq 1 \tag{23}$$

$$\begin{aligned} x_{12} + x_{13} - x_{23} &\leq 1 \\ x_{12} - x_{13} + x_{23} &\leq 1 \end{aligned} \tag{24}$$

with Eq. (23) corresponding to $\tilde{\mathbf{N}}_t$. Hence, $\text{vol}(\tilde{\mathbf{N}}_t) = 1$. The V -representation for $\tilde{\mathbf{L}}_t$ is easily obtained:

$$\tilde{\mathbf{L}}_t = \text{conv} \left\{ (0, 0, 0), (1, 1, 1), (1, 0, 0), (0, 1, 0), (0, 0, 1), (0, 1, 1) \right\}.$$

This region is plotted in Figure 4.

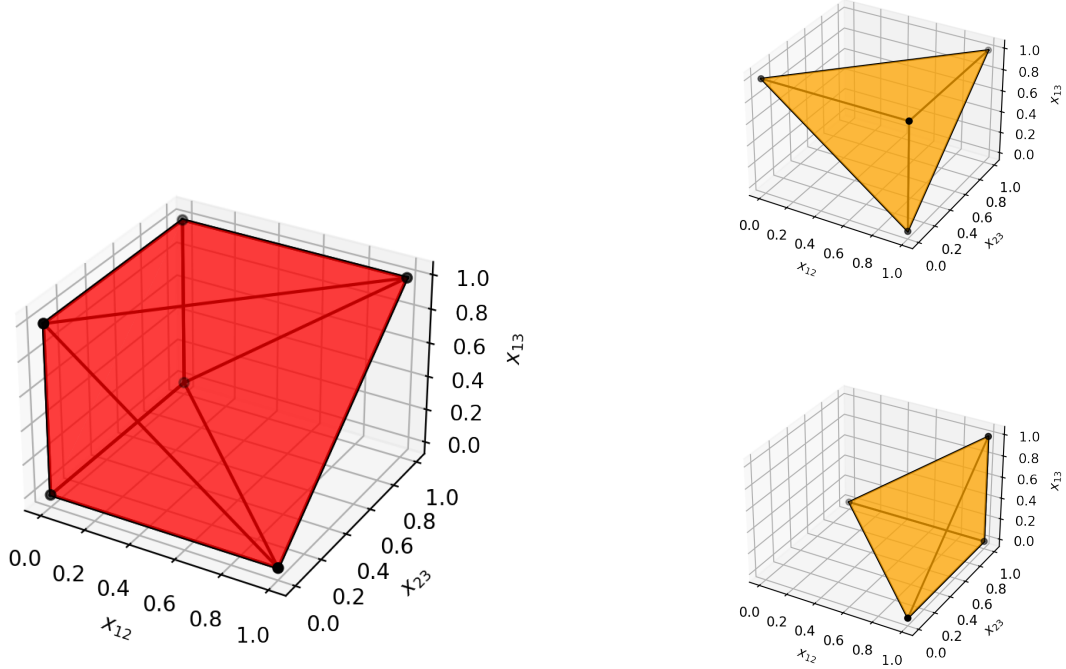


FIGURE 4. The scaled local polytope slice \tilde{L}_t , for $0 < t \leq 1/6$ (left). In the right panel, we show the two triangular pyramids removed from the unit cube to obtain figure on the left.

Both $\text{conv}\{(1, 0, 0), (0, 0, 1), (1, 1, 1), (1, 0, 1)\}$ and $\text{conv}\{(1, 0, 0), (0, 0, 1), (1, 1, 1), (1, 1, 0)\}$ are triangular pyramids with volume $1/6$ as can be seen in figure 4. The scaled slice L_t is just the unit cube with these two regions removed. Hence,

$$\forall t \in (0, 1/6] \quad \text{vol}(\tilde{L}_t) = 1 - 2 \cdot \frac{1}{6} = \frac{2}{3} \quad (25)$$

Next, we look at the region $t \in (1/6, 1/4]$. The relevant inequalities for the H -representation of \tilde{N}_t are given by Eq. (23). Hence, $\text{vol}(\tilde{N}_t) = 1$.

The H -representation of the local slice \tilde{L}_t are the inequalities in Eq. (23) and (22b)-(22d). The corresponding V -representation is

$$\text{conv}\{(0, 0, 0), (1, 1, 1), (1, 0, 0), (0, 1, 0), (0, 0, 1), (0, 1, k_1), (0, k_1, 1), (k_2, 1, 1)\},$$

where $k_1 = 1/(2t) - 2$ and $k_2 = 3 - 1/(2t)$. This region is plotted in Fig. 5.

The volume of the local slice now is just the volume of the local slice obtained for $t \in (0, 1/6]$ minus the volume of the yellow region. The yellow region is a triangular pyramid scaled by $3 - 1/(2t)$ and hence the volume is given by:

$$V_{\text{yellow}} = \frac{(3 - 1/(2t))^3}{6}$$

Hence, we have:

$$\forall t \in (1/6, 1/4] \quad \text{vol}(\tilde{L}_t) = \frac{2}{3} - \frac{(3 - 1/(2t))^3}{6} \quad (26)$$

For the values $t \in (1/4, 1/2]$, we look back at inequalities in Eqs. (21) and (22) and use the substitution $q_{12} = tx_{12}$, $q_{23} = (1/2 - t)x_{23}$ and $q_{13} = (1/2 - t)x_{13}$. The resulting inequalities are:

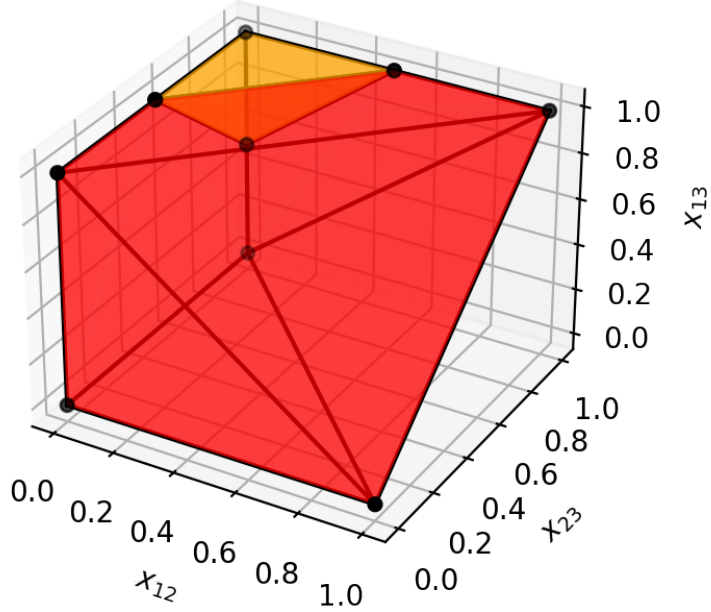


FIGURE 5. The scaled local polytope slice $\tilde{\mathbf{L}}_t$, for $1/6 < t \leq 1/4$ (in red). The yellow region represents the difference between this case and the case when $t \leq 1/6$, see Fig. 4.

$$0 \leq x_{ij} \leq 1 \quad (27)$$

$$\begin{aligned} x_{12} + \left(\frac{1}{2t} - 1\right)x_{13} - \left(\frac{1}{2t} - 1\right)x_{23} &\leq 1 \\ x_{12} - \left(\frac{1}{2t} - 1\right)x_{13} + \left(\frac{1}{2t} - 1\right)x_{23} &\leq 1 \\ -x_{12} + \left(\frac{1}{2t} - 1\right)x_{13} + \left(\frac{1}{2t} - 1\right)x_{23} &\leq \frac{1}{2t} - 1 \end{aligned} \quad (28)$$

In this new substitution, $\text{vol}(\tilde{\mathbf{N}}_t)$ is unity again. The V -representation of $\tilde{\mathbf{L}}_t$ is

$$\text{conv} \left\{ (0, 0, 0), (1, 1, 1), (1, 0, 0), (0, 1, 0), (0, 0, 1), (1, 1, 1), \right. \\ \left. (1/(2t) - 1, 1, 1), (2 - 1/(2t), 1, 0), (2 - 1/(2t), 0, 1) \right\}$$

We plot this region in Fig. 6.

It is easy to see that the local slice $\tilde{\mathbf{L}}_t$ is the unit cube minus the 3 triangular pyramids (shaded yellow) of base area $1/2$, height $1/(2t) - 1$ and hence of volume,

$$V_{\text{yellow}} = \frac{1}{3} \cdot \frac{1}{2} \cdot \left(\frac{1}{2t} - 1\right) = \frac{1/(2t) - 1}{6}$$

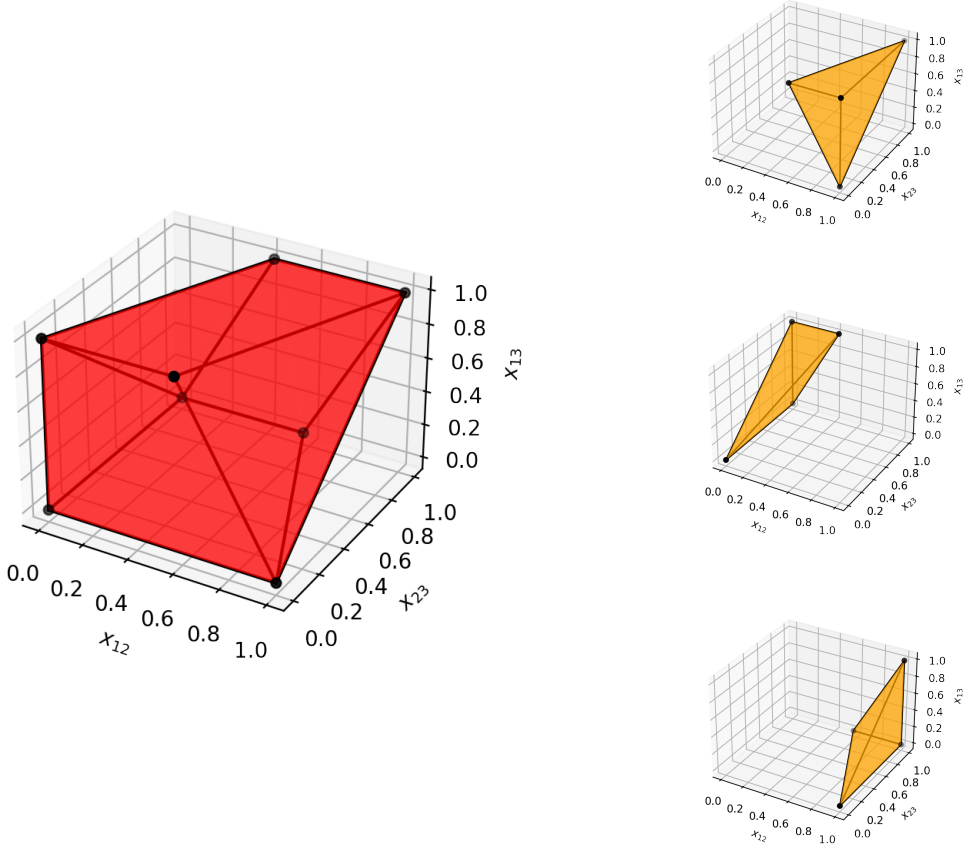


FIGURE 6. The scaled local polytope slice $\tilde{\mathbf{L}}_t$, for $1/4 < t \leq 1/2$ (left). In the right panel, we show the three triangular pyramid regions removed from the unit cube to get figure on the left.

Hence, we have:

$$\forall t \in (1/4, 1/2] \quad \text{vol}(\tilde{\mathbf{L}}_t) = 1 - \frac{(1/(2t) - 1)}{2} \quad (29)$$

Proposition 6.3. *The volume ratio of skewed slices ($p_1 = p_2 = t$, $p_3 = 1/2 - t$) between the local and no-signaling polytopes corresponding to the triangle graph K_3 are given by (see Fig. 7):*

$$\frac{\text{vol}(\mathbf{L}_t)}{\text{vol}(\mathbf{N}_t)} = \begin{cases} \frac{2}{3}, & t \in (0, \frac{1}{6}] \\ \frac{2}{3} - \frac{(3 - 1/(2t))^3}{6}, & t \in (\frac{1}{6}, \frac{1}{4}] \\ 1 - \frac{(1/(2t) - 1)}{2}, & t \in (\frac{1}{4}, \frac{1}{2}) \end{cases}$$

7. THE SQUARE GRAPH

In this section, we analyze in detail the case of $K_{2,2}$ which is the complete-bipartite graph. As explained in Section 4, this case corresponds to the famous CHSH scenario [CHSH69], and more generally 2-player non-local games with 2 questions and 2 answers. In this work we are focusing only on the local and non-signaling sets of correlations; for an in-depth study of the set of *quantum* correlations, we refer the reader to the excellent work [LMS⁺23]. Note that we embed below the graph $K_{2,2}$ in the plane as a square, see also Section 8 for the discussion of arbitrary cycle graphs.

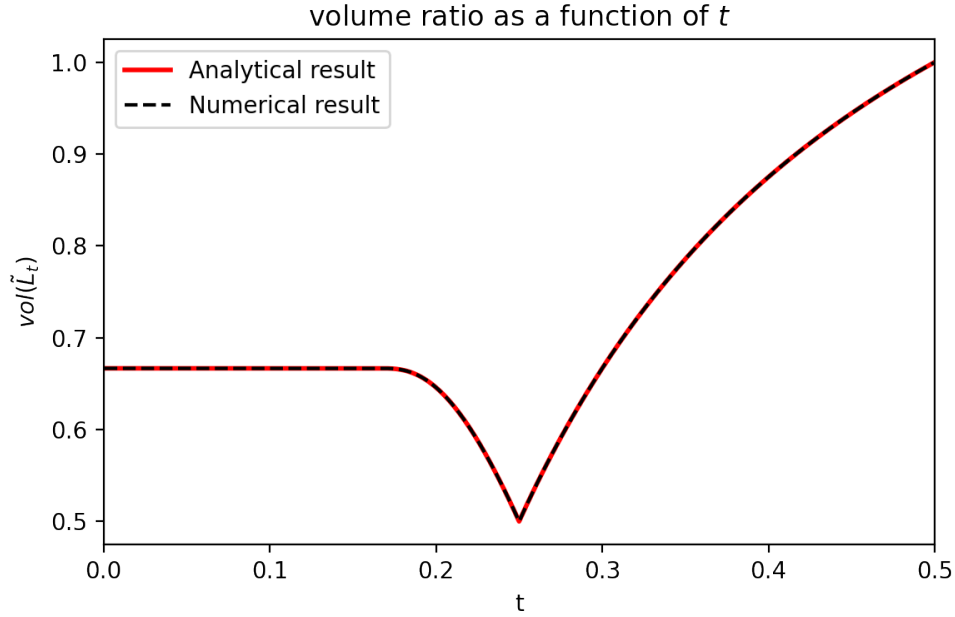
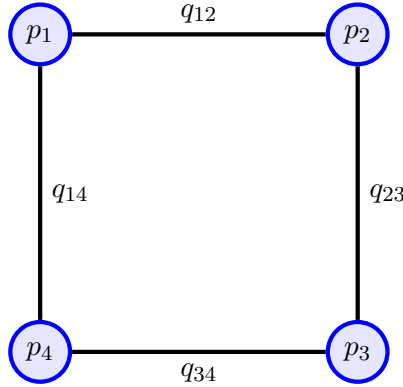


FIGURE 7. Volume ratio between the local polytope slice and the non-signaling polytope slice, in the skewed ($p_1 = p_2 = t, p_3 = 1/2 - t$) case.



The V -representation of $L(K_{2,2}) = \text{COR}(K_{2,2})$ is given by the convex hull of all rows of the truth table presented in Table 2. This is then used to obtain the H -representation below:

$$\begin{aligned} 0 \leq q_{ij} &\leq \min(p_i, p_j) \\ p_i + p_j - p_{ij} &\leq 1 \end{aligned} \tag{30}$$

$$\begin{aligned} 0 \leq p_3 + p_4 + q_{12} - q_{23} - q_{34} - q_{14} &\leq 1 \\ 0 \leq p_1 + p_4 - q_{12} + q_{23} - q_{34} - q_{14} &\leq 1 \\ 0 \leq p_1 + p_2 - q_{12} - q_{23} + q_{34} - q_{14} &\leq 1 \\ 0 \leq p_2 + p_3 - q_{12} - q_{23} - q_{34} + q_{14} &\leq 1 \end{aligned} \tag{31}$$

The polytopes in question in this case are 8-dimensional corresponding to 4 each of vertices (p_i) and edges (q_{ij}).

$$L(K_{2,2}) = \text{COR}(K_{2,2}) \subseteq N(K_{2,2}) = \text{TRA}(K_{2,2}) \subset \mathbb{R}^8$$

| V-part | | | | E-part | | | |
|--------|---|---|---|--------|----|----|----|
| 1 | 2 | 3 | 4 | 12 | 23 | 34 | 14 |
| 0 | 0 | 0 | 0 | 0 | 0 | 0 | 0 |
| 0 | 0 | 0 | 1 | 0 | 0 | 0 | 0 |
| 0 | 0 | 1 | 0 | 0 | 0 | 0 | 0 |
| 0 | 0 | 1 | 1 | 0 | 0 | 1 | 0 |
| 0 | 1 | 0 | 0 | 0 | 0 | 0 | 0 |
| 0 | 1 | 0 | 1 | 0 | 0 | 0 | 0 |
| 0 | 1 | 1 | 0 | 0 | 1 | 0 | 0 |
| 0 | 1 | 1 | 1 | 0 | 1 | 1 | 0 |

| V-part | | | | E-part | | | |
|--------|---|---|---|--------|----|----|----|
| 1 | 2 | 3 | 4 | 12 | 23 | 34 | 14 |
| 1 | 0 | 0 | 0 | 0 | 0 | 0 | 0 |
| 1 | 0 | 0 | 1 | 0 | 0 | 0 | 1 |
| 1 | 0 | 1 | 0 | 0 | 0 | 0 | 0 |
| 1 | 0 | 1 | 1 | 0 | 0 | 1 | 1 |
| 1 | 1 | 0 | 0 | 1 | 0 | 0 | 0 |
| 1 | 1 | 0 | 1 | 1 | 0 | 0 | 1 |
| 1 | 1 | 1 | 0 | 1 | 1 | 0 | 0 |
| 1 | 1 | 1 | 1 | 1 | 1 | 1 | 1 |

TABLE 2. V -representation of $L(K_{2,2})$, split in two tables.

Inequalities in Eq. (30) correspond to $N(K_{2,2})$ while inequalities in Eq. (31) are the additional constraints defining $L(K_{2,2})$; these are the *Bell inequalities*. The volume of these polytopes is given by [LS20]:

$$\text{vol}(N(K_{2,2})) = \frac{17}{10800} \quad \text{and} \quad \text{vol}(L(K_{2,2})) = \frac{1}{630} = \frac{16}{17} \text{vol}(N(K_{2,2})).$$

We set $p_1 = p_2 = p_3 = p_4 = t \in (0, 1]$ and study the slices $L(p = (t, t, t, t), K_{2,2})$ and $N(p = (t, t, t, t), K_{2,2})$. The corresponding H -representation for $L(p = (t, t, t, t), K_{2,2})$ reads:

$$\max\{0, 2t - 1\} \leq q_{ij} \leq t \tag{32}$$

$$\begin{aligned} -2t &\leq q_{12} - q_{23} - q_{34} - q_{14} \leq 1 - 2t \\ -2t &\leq -q_{12} + q_{23} - q_{34} - q_{14} \leq 1 - 2t \\ -2t &\leq -q_{12} - q_{23} + q_{34} - q_{14} \leq 1 - 2t \\ -2t &\leq -q_{12} - q_{23} - q_{34} + q_{14} \leq 1 - 2t \end{aligned} \tag{33}$$

As before, we define our polytopes of interest by:

$$\begin{aligned} N_t &:= N(p = (t, t, t, t), K_{2,2}) = \{(q_{12}, q_{23}, q_{34}, q_{14}) \in \mathbb{R}^4 : \text{Eq. (32) holds}\} \\ L_t &:= L(p = (t, t, t, t), K_{2,2}) = \{(q_{12}, q_{23}, q_{34}, q_{14}) \in \mathbb{R}^4 : \text{Eq. (32) and Eq. (33) hold}\}. \end{aligned}$$

We'll focus only in the range $t \in (0, 1/2]$ owing to Proposition 6.1. Setting $q_{ij} = tx_{ij}$, we finally have:

$$0 \leq x_{ij} \leq 1 \tag{34}$$

$$\begin{aligned}
x_{12} - x_{23} - x_{34} - x_{14} &\leq \frac{1}{t} - 2 \\
-x_{12} + x_{23} - x_{34} - x_{14} &\leq \frac{1}{t} - 2 \\
-x_{12} - x_{23} + x_{34} - x_{14} &\leq \frac{1}{t} - 2 \\
-x_{12} - x_{23} - x_{34} + x_{14} &\leq \frac{1}{t} - 2
\end{aligned} \tag{35}$$

$$\begin{aligned}
-x_{12} + x_{23} + x_{34} + x_{14} &\leq 2 \\
x_{12} - x_{23} + x_{34} + x_{14} &\leq 2 \\
x_{12} + x_{23} - x_{34} + x_{14} &\leq 2 \\
x_{12} + x_{23} + x_{34} - x_{14} &\leq 2
\end{aligned} \tag{36}$$

Following the previous section we define our scaled polytopes:

$$\begin{aligned}
\tilde{\mathbf{N}}_t &:= \{(x_{12}, x_{23}, x_{34}, x_{14}) \in \mathbb{R}^4 : \text{Eq. (34) holds}\} \\
\tilde{\mathbf{L}}_t &:= \{(x_{12}, x_{23}, x_{34}, x_{14}) \in \mathbb{R}^4 : \text{Eq. (34) and Eq. (36) hold}\}.
\end{aligned}$$

Since, $\text{vol}(\mathbf{N}_t) = t^4 \text{vol}(\tilde{\mathbf{N}}_t)$, and similarly for the local polytope; we have,

$$\frac{\text{vol}(\mathbf{L}_t)}{\text{vol}(\mathbf{N}_t)} = \frac{\text{vol}(\tilde{\mathbf{L}}_t)}{\text{vol}(\tilde{\mathbf{N}}_t)}.$$

From inequalities in Eq. (34), we see $\tilde{\mathbf{N}}_t$ is the 4-D unit cube $[0, 1]^4$ with volume given by $\text{vol}(\tilde{\mathbf{N}}_t) = 1$ independent of t . Next, we notice that inequalities (35) are trivially satisfied for all $t \in (0, 1/3]$ while the inequalities in Eq. (36) are independent of t .

Hence, we will start by looking at $t \in (0, 1/3]$, where the only relevant inequalities in the H -representation of $\tilde{\mathbf{L}}_t$ are (34) and (36). The V -representation is thus given by the convex hull of the following 12 vertices:

$$\begin{aligned}
(0, 0, 0, 0), (1, 0, 0, 0), (0, 1, 0, 0), (0, 0, 1, 0), (0, 0, 0, 1), (1, 1, 0, 0), \\
(1, 0, 1, 0), (1, 0, 0, 1), (0, 1, 1, 0), (0, 1, 0, 1), (0, 0, 1, 1), (1, 1, 1, 1)
\end{aligned}$$

We note that these are all the vertices of a tesseract but with permutations of $(1, 1, 1, 0)$ removed. Removing each of these permutation amounts to the removal of a 4-simplex. Using the fact that the volume of an n -simplex is given by $1/n!$, we have:

$$\forall t \in \left(0, \frac{1}{3}\right] \quad \text{vol}(\tilde{\mathbf{L}}_t) = 1 - 4 \cdot \frac{1}{4!} = \frac{5}{6}. \tag{37}$$

Next, looking in the range $t \in (1/2, 1/3]$, the inequalities (35) start cutting in and the V -representation for \tilde{L}_t is given by,

$$\text{conv} \left\{ (0, 0, 0, 0) \right. \\ \left. \left(\frac{1}{t} - 2, 0, 0, 0 \right), \left(1, 3 - \frac{1}{t}, 0, 0 \right), \left(1, 0, 3 - \frac{1}{t}, 0 \right), \left(1, 0, 0, 3 - \frac{1}{t} \right) \right. \\ \left. \left(0, \frac{1}{t} - 2, 0, 0 \right), \left(3 - \frac{1}{t}, 1, 0, 0 \right), \left(0, 1, 3 - \frac{1}{t}, 0 \right), \left(0, 1, 0, 3 - \frac{1}{t} \right) \right. \\ \left. \left(0, 0, \frac{1}{t} - 2, 0 \right), \left(3 - \frac{1}{t}, 0, 1, 0 \right), \left(0, 3 - \frac{1}{t}, 1, 0 \right), \left(0, 0, 1, 3 - \frac{1}{t} \right) \right. \\ \left. \left(0, 0, 0, \frac{1}{t} - 2 \right), \left(3 - \frac{1}{t}, 0, 0, 1 \right), \left(0, 3 - \frac{1}{t}, 0, 1 \right), \left(0, 0, 3 - \frac{1}{t}, 1 \right) \right. \\ \left. (1, 1, 0, 0), (1, 0, 1, 0), (1, 0, 0, 1), (0, 1, 1, 0), (0, 1, 0, 1), (0, 0, 1, 1), (1, 1, 1, 1) \right\}$$

We observe that each of the inequalities in (35) splits each permutation of $(1, 0, 0, 0)$ into 4 vertices amounting to a removed volume equivalent to a 4-simplex scaled by $3 - 1/t$. Thus, we have:

$$\forall t \in \left(\frac{1}{3}, \frac{1}{2} \right] \quad \text{vol}(\tilde{L}_t) = \frac{5}{6} - 4 \cdot \frac{1}{4!} \cdot \left(3 - \frac{1}{t} \right)^4 = \frac{5 - (3 - 1/t)^4}{6} \quad (38)$$

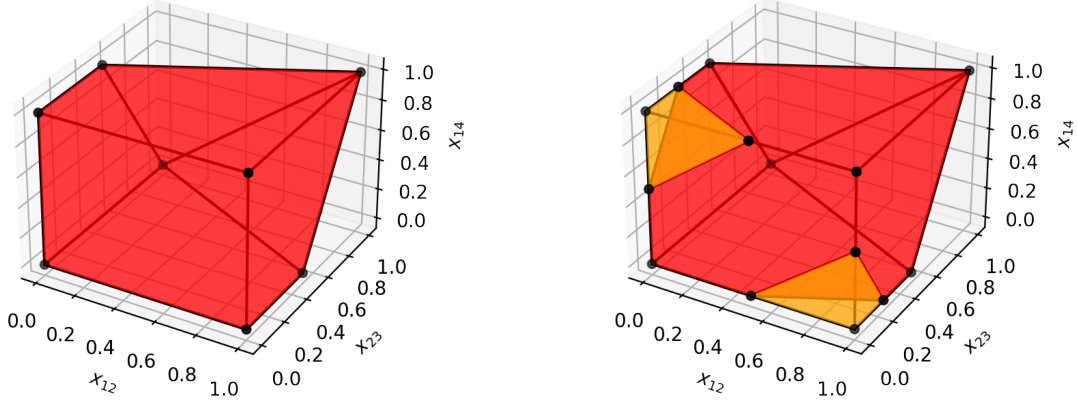


FIGURE 8. The $x_{23} = x_{34}$ slices of $L(p, K_{2,2})$. Left: $t \in (0, \frac{1}{3}]$. Right: $t = 0.4$; the yellow sections are the volumes removed due to inequalities (35).

Thus, combining the results of this section, we obtain our main result. This is plotted against numerical result in Figure 9.

Proposition 7.1. *The volume ratio of slices ($p_1 = p_2 = p_3 = p_4 = t$) between the local and the non-signaling polytopes corresponding to the complete-bipartite graph $K_{2,2}$ is given by:*

$$\frac{\text{vol}(\mathbf{L}_t)}{\text{vol}(\mathbf{N}_t)} = \begin{cases} \frac{5}{6}, & t \in (0, \frac{1}{3}] \\ \frac{5 - (3 - 1/t)^4}{6}, & t \in (\frac{1}{3}, \frac{1}{2}] \\ \frac{5 - (3 - 1/(1-t))^4}{6}, & t \in (\frac{1}{2}, \frac{2}{3}] \\ \frac{5}{6}, & t \in (\frac{1}{3}, 1] \end{cases}$$

The various parameters as defined in Section 5 are:

$$\begin{aligned} \text{The fall-off value } \tau(K_{2,2}) &= \frac{1}{3} \\ \text{The initial ratio } \rho_{0+}(K_{2,2}) &= \frac{5}{6} \\ \text{The middle ratio } \rho_{1/2}(K_{2,2}) &= \frac{2}{3}. \end{aligned}$$

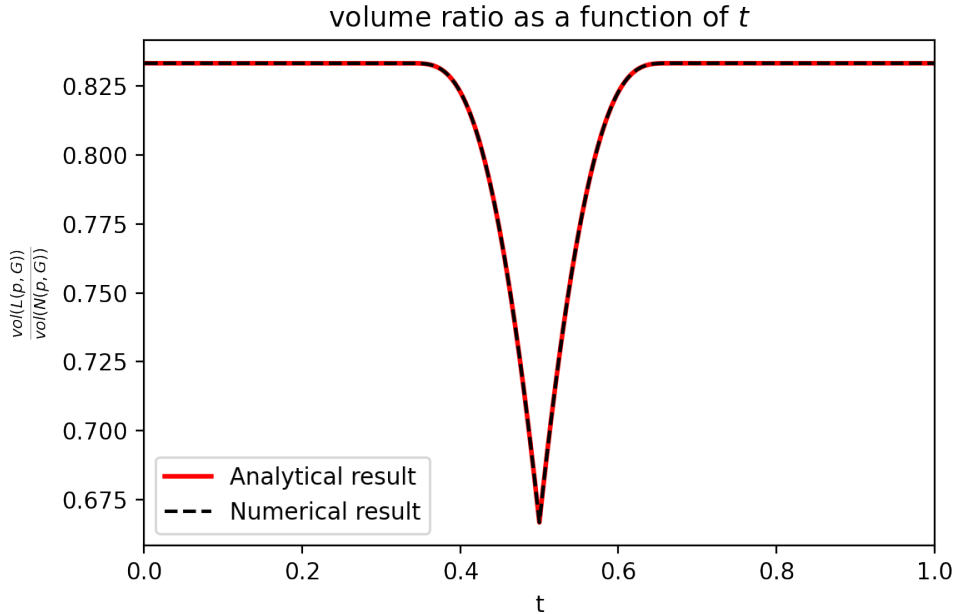


FIGURE 9. $\frac{\text{vol}(L(p, K_{2,2}))}{\text{vol}(N(p, K_{2,2}))}$ as a function of t

In terms of the CHSH game, Proposition 7.1 can be interpreted as follows. Consider Alice and Bob sharing a randomly sampled no-signaling box with the condition that the marginal distribution of each of their own questions are fixed to be t . In such a case, the highest probability of the randomly sampled box being non-local occurs when $t = 1/2$. In fact, the $t = 1/2$ value is interesting in its own right, as many important behaviours such as the PR boxes [PR94] and the boxes corresponding to maximal quantum violations (where Alice and Bob share a maximally entangled Bell state) all lie on this slice.

8. CYCLE GRAPHS

In the previous two sections, we have discussed in great detail the cases of the triangle graph K_3 and that of the complete bipartite graph $K_{2,2}$. These are *cycle graphs*, $K_3 = C_3$ and $K_{2,2} = C_4$. Another well-studied cyclic scenario often found in literature is the KCBS [KCBS08] scenario which corresponds to C_5 . Physically this is equivalent to measuring the two components of a bipartite system along five distinct measurement directions (5 questions) each yielding two possible outcomes (2 answers each). We would not study C_5 specifically but rather in this section, we shall establish some general results for cycle graphs of arbitrary order C_n . Our analysis builds on the work of Araújo, Túlio Quintino, Budroni, Terra Cunha, and Cabello [AQB⁺13], in which the facets of $L(C_n)$ have been described. and we will use them to derive general results for the volume of slices $L(C_n, p = (t, \dots, t))$ and $N(C_n, p = (t, \dots, t))$.

Proposition 8.1 ([AQB⁺13, Theorem 1]). *For a set of observables $\{X_0, X_1, \dots, X_{n-1}\}$, all the 2^{n-1} tight noncontextuality inequalities for the n -cycle noncontextual polytope are*

$$\sum_{i=0}^{n-1} \gamma_i \langle X_i X_{i+1} \rangle \leq n - 2, \quad (39)$$

where $\gamma_i = \pm 1$ are such that there are odd number of -1 's.

Here, $\langle X_i X_{i+1} \rangle = 4q_{ij} - 2p_i - 2p_j + 1$, the non-contextual inequalities in the H -representation of $L(C_n)$ are given by:

$$4 \sum_{i=0}^{n-1} \gamma_i q_{i,i+1} - 2 \sum_i^{n-1} \gamma_i (p_i + p_{i+1}) + \sum_i^{n-1} \gamma_i \leq n - 2 \quad (40)$$

We can get the corresponding noncontextuality inequalities for the slice $L(C_n)_t := L(p = \{t, \dots, t\}, C_n)$ by just substituting $p = \{t, \dots, t\}$ in (40).

Definition 8.2. *For $p = \{t, \dots, t\}$, we define the m -negative inequality for $L(p = \{t, \dots, t\}, C_n)$ as the inequality with $\gamma_i = -1$ for m values. Note that m can only take odd values for valid noncontextuality inequalities. Thus, the m -negative inequalities, after substituting $q_{ij} = tx_{ij}$ are given by:*

$$\sum_{i=0}^{n-1} \gamma_i x_{ij} \leq \frac{m-1}{2t} + n - 2m \quad (41)$$

The remaining inequalities in the H -representation of $L(C_n)_t$ are of the form given in Eq. (11) corresponding to $N(C_n)_t$. Under the substitution $p_{ij} = tx_{ij}$ and $t \in \left(0, \frac{1}{2}\right]$ these are again of the form:

$$0 \leq x_{ij} \leq 1 \quad (42)$$

Denoting the polytopes of interest again by:

$$\begin{aligned} \tilde{N}_t &:= \{(x_{12}, x_{23}, \dots, x_{1n-1}) \in \mathbb{R}^n : \text{Eq. (42) holds}\} \\ \tilde{L}_t &:= \{(x_{12}, x_{23}, \dots, x_{1n-1}) \in \mathbb{R}^n : \text{Eq. (42) and Eq. (41) hold}\}. \end{aligned}$$

Again, it is straightforward to see that \tilde{N}_t is the unit cube $[0, 1]^n$. We will now look at how the m -inequalities cut into this cube to give shape to \tilde{L}_t . We start by noting the the 1-negative inequalities are independent of t . The RHS of inequality (41) becomes $n - 2$ for $m = 1$. This implies that the vertices of the cube with $n - 1$ number of 1s are no longer part of \tilde{L}_t . In fact, the resultant body formed after imposing 1-negative constraint on \tilde{N}_t is just the convex hull of the remaining vertices of the cube.

Proposition 8.3. *The volume removed by 1-negative inequalities from \tilde{N}_t is $\frac{1}{n!}$.*

This is because each 1-negative inequality removes a n -simplex from the cube.

Proposition 8.4. *Any m -negative inequality is trivially satisfied for all $t \in \left[0, \frac{m-1}{2m}\right]$.*

This is clear if one notices that maximum value the right hand side of eqn 41 can take is $n - m$.

Proposition 8.5. *For $m \geq 2$, an m -inequality starts cutting into \tilde{N}_t by splitting the points of form*

$$\text{perm}(\underbrace{1, 1, \dots, 1}_{n-m \text{ times}}, \underbrace{0, 0, \dots, 0}_{m \text{ times}})$$

into n points. These n points correspond to either one 0 being replaced by $m - \frac{m-1}{2t}$ or one 1 being replaced by $1 - m + \frac{m-1}{2t}$.

Proposition 8.6. For $m \geq 2$ and $t \geq \frac{m-1}{2m}$, the volume removed by an m -inequality from $\tilde{\mathbf{N}}_t$ is

$$\frac{1}{n!} \cdot \left(m - \frac{m-1}{2t}\right)^n$$

This follows from Proposition 8.5 as the region removed is just a n -simplex scaled by $m - \frac{m-1}{2t}$. Next, we notice that for $t = \frac{1}{2}$, $m - \frac{m-1}{2t} = 1$ and hence, an m -inequality takes points with m (odd) number of 1s to $m-1$ (even) or $m+1$ (even) number of 1s.

Proposition 8.7. For $t = 1/2$, $\tilde{\mathbf{L}}_t$ is demicube with volume given by:

$$\text{vol}(\tilde{\mathbf{L}}_t) = 1 - \frac{2^{n-1}}{n!}.$$

These results completely define the structure of $\text{vol}(\tilde{\mathbf{L}}_{t=1/2})/\text{vol}(\tilde{\mathbf{N}}_t)$.

Proposition 8.8. The ratio of volumes of symmetric slices for C_n is given by the following results. for $t \in (0, 1/2]$

$$\frac{\text{vol}(\mathbf{L}(p = (t, \dots, t), C_n))}{\text{vol}(\mathbf{L}(p = (t, \dots, t), C_n))} = \frac{\text{vol}(\tilde{\mathbf{L}}_t)}{\text{vol}(\tilde{\mathbf{N}}_t)} = \begin{cases} 1 - \sum_{k=1}^m \frac{1}{n!} \binom{n}{n-k} \left(k - \frac{k-1}{2t}\right)^n & n - m > 1, t \in \left(\frac{m-1}{2m}, \frac{m+1}{2(m+2)}\right] \\ 1 - \sum_{k=1}^m \frac{1}{n!} \binom{n}{n-k} \left(k - \frac{k-1}{2t}\right)^n & n - m \leq 1, t \in \left(\frac{m-1}{2m}, \frac{1}{2}\right] \end{cases}$$

where m must be an odd number not greater than n and k only takes odd values in the sum.

Proposition 8.9. For the cycle graphs C_n ($n \geq 3$), the various volume ratio parameters defined in Section 5 are:

$$\text{The fall-off value } \tau(C_n) = \frac{1}{3}$$

$$\text{The initial ratio } \rho_{0+}(C_n) = 1 - \frac{1}{(n-1)!}$$

$$\text{The middle ratio } \rho_{1/2}(C_n) = 1 - \frac{2^{n-1}}{n!}.$$

The ratio $\text{vol} \mathbf{L}(C_n)/\text{vol} \mathbf{N}(C_n)$ goes to unity in the $n \rightarrow \infty$ as already shown in [LS20]. From 8.8, we see the same happens for the symmetric slices and the ratio $\text{vol} \mathbf{L}_t/\text{vol} \mathbf{N}_t$ goes to 1 as $n \rightarrow \infty$. We plot this volume ratio for C_n for different values of n in Fig. 10.

9. THE COMPLETE GRAPH ON FOUR VERTICES

We now shift our attention to K_4 , the complete graph on four vertices, see Fig. 11. In Section 10, we shall see that the inequalities for any graph with $|V|$ vertices can be obtained from the inequalities of $K_{|V|}$, hence the importance of the study of complete graphs.

Before we start, let us recall the *Inclusion-Exclusion* inequalities. For a set of events $\{A_i : 1 \leq i \leq n\}$ we have associated probabilities $\{p_i = P(A_i) : 1 \leq i \leq n\}$ and, more generally,

$$\{p_{i_1 i_2 \dots i_k} = P(A_{i_1} \cup A_{i_2} \cup \dots \cup A_{i_k}) : 1 \leq i_1, \dots, i_k \leq n, N \leq n\}$$

as well as

$$\{q_{i_1 i_2 \dots i_k} = P(A_{i_1} \cap A_{i_2} \cap \dots \cap A_{i_k}) : 1 \leq i_1, \dots, i_k \leq n\}.$$

Then the Inclusion-Exclusion inequalities are given by:

$$p_{i_1 i_2 \dots i_k} = \sum_{r=1}^N (-1)^{r+1} \sum_{j_1, \dots, j_r \in \{i_1, \dots, i_k\}} q_{j_1 \dots j_r} \geq 0, \quad (43)$$

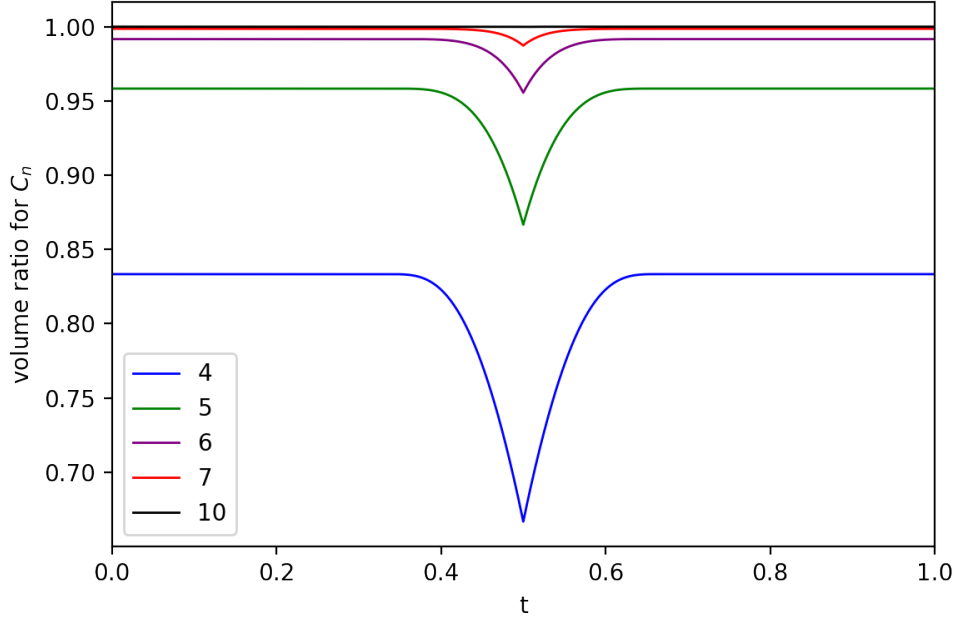


FIGURE 10. The volume ratio $\text{vol } L_t / \text{vol } N_t$ plotted as a function of t for C_n . The legend shows the value of n for each plot. We see that as n increases, the volume ratio tends to 1.

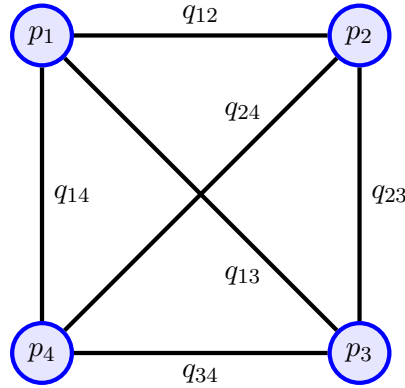


FIGURE 11. The K_4 graph

with $q_i = p_i$ in the expansion. Now, since in our case, we do not deal with hypergraphs, we are limited to an intersection of maximum two events (recall that contexts are of maximum size 2). Thus, we modify the Inclusion-Exclusion inequality in our case as :

$$p_{i_1 i_2 \dots i_k} = \sum_{r=1}^2 (-1)^{r+1} \sum_{j_1, \dots, j_r \in \{i_1, \dots, i_k\}} q_{j_1 \dots j_r} \geq 0. \quad (44)$$

We start by recalling a general result about complete graphs.

Proposition 9.1. [Pit91, Theorem 2.2] *For any graph complete graph $K_{|V|}$ with $|V| \geq 2$, the Inclusion-Exclusion inequalities form facets of $\mathbb{L}(K_{|V|})$.*

These are not all the facets of $K_{|V|}$ in general as pointed in [Pit91] with the Chung inequalities [Chu41] being an example of other possible facets.

Proposition 9.2. *For K_4 , the Inclusion-Exclusion inequalities along with the no-disturbance inequalities give all the facets.*

This was conjectured by Pitowsky himself and we have checked this with `cdd` [Fuk23]. Hence, once we have all the inequalities in the H -representation of $L(K_4)$ from Proposition 9.2, we can start studying our sliced polytopes.

Let us list down the inequalities of $L(K_4, p = (t, t, t, t))$ ordering them on the basis of the value of t , they become active at. In what proceeds, $i, j, k, l \in \{1, 2, 3, 4\}$ are distinct.

The inequalities cutting in from $t = 0$ are:

$$\begin{aligned} -q_{ij} &\leq 0 \\ q_{ij} &\leq t \end{aligned} \tag{45}$$

which we get from the no-disturbance condition. We also have the inequality $-p_{ij} \leq 1 - 2t$ but that is not relevant for $0 \leq t \leq 1/2$. The remaining inequalities can be obtained from the Inclusion-Exclusion conditions.

$$\begin{aligned} -q_{jk} + q_{ij} + q_{ik} &\leq t \\ q_{ij} + q_{ik} + q_{il} - q_{jk} - q_{jl} - q_{kl} &\leq t \\ -q_{ij} - q_{kl} + q_{ik} + q_{il} + q_{jk} + q_{jl} &\leq 2t \end{aligned} \tag{46}$$

The inequalities cutting in from $t = 1/4$ are:

$$\begin{aligned} -q_{ij} - q_{ik} - q_{il} - q_{jk} - q_{jl} - q_{kl} &\leq 1 - 4t \\ -q_{ij} - q_{ik} - q_{jk} + q_{jl} + q_{il} + q_{kl} &\leq 1 - t \end{aligned} \tag{47}$$

The inequalities cutting in from $t = 1/3$ are:

$$-q_{ij} - q_{ik} - q_{jk} \leq 1 - 3t \tag{48}$$

The inequalities cutting in from $t = 3/8$ are:

$$-q_{ij} - q_{ik} - q_{jk} - q_{jl} - q_{il} - q_{kl} \leq 3 - 8t \tag{49}$$

We define the polytopes of interest:

$$\begin{aligned} N_t &:= N(p = (t, t, t, t), K_4) = \{(q_{12}, q_{23}, q_{34}, q_{14}, q_{13}, q_{24}) \in \mathbb{R}^6 : \text{Eq. (45) holds}\} \\ L_t &:= L(p = (t, t, t, t), K_4) = \{(q_{12}, q_{23}, q_{34}, q_{14}, q_{13}, q_{24}) \in \mathbb{R}^6 : \text{Eq. (45)-(49) hold}\}. \end{aligned}$$

Let us now look at the various parameters for K_4 .

Proposition 9.3. *Since, the first inequalities cutting in at a non-zero t value are given by the inequalities 47, the fall of value for K_4 is given by:*

$$\tau(K_4) = \frac{1}{4}.$$

In the region $0 \leq t \leq 1/4$, the relevant inequalities in the H -representation of L_t are 45 and 46. The corresponding V -representation is:

$$\begin{aligned} \text{conv} \left\{ (0, 0, 0, 0, 0, 0), (t, t, 0, t, 0, 0), (t, 0, t, 0, t, 0), (0, t, t, 0, 0, t), (0, 0, 0, t, t, t) \right. \\ (0, t, 0, 0, t, 0), (0, 0, t, t, 0, 0), (t, 0, 0, 0, 0, t), (t, 0, 0, 0, 0, 0), (0, t, 0, 0, 0, 0) \\ \left. (0, 0, t, 0, 0, 0), (0, 0, 0, t, 0, 0), (0, 0, 0, 0, t, 0), (0, 0, 0, 0, 0, t), (t, t, t, t, t, t) \right\} \end{aligned}$$

The volume of N_t is simply t^6 . The volume of L_t can be computed (numerically, using `cdd`) from the convex hull.

Proposition 9.4. *The initial ratio for K_4 is given by :*

$$\rho_{0+}(K_4) = \frac{5}{36}.$$

Finally, for $t = 1/2$, the H -representation of L_t has all the inequalities in (45)-(49). The V -representation reads:

$$\text{conv} \left\{ (0.5, 0, 0, 0, 0, 0.5), (0, 0.5, 0, 0, 0.5, 0), (0, 0, 0.5, 0.5, 0, 0), (0.5, 0.5, 0, 0.5, 0, 0), \right. \\ (0.5, 0, 0.5, 0, 0.5, 0), (0.5, 0.5, 0, 0.5, 0, 0), (0.5, 0, 0.5, 0, 0.5, 0), (0, 0.5, 0.5, 0, 0, 0.5), \\ \left. (0, 0, 0, 0.5, 0.5, 0.5), (0.5, 0.5, 0.5, 0.5, 0.5, 0.5) \right\}.$$

The volume of this region is $1/1440$ while the volume of N_t is just $1/2^6$.

Proposition 9.5. *The middle ratio for K_4 is given by:*

$$\rho_{1/2}(K_4) = \frac{2}{45}.$$

Finally, we provide the computationally obtained plot for t against the volume ratio in Fig. 15.

10. OPERATIONS ON GENERAL GRAPHS

To obtain the H -representation of the local polytope $L(G) = \text{COR}(G)$, the obvious method is to list down the V -representation using the truth-table approach from Definition 3.1 and solve the convex hull problem. However, there are other approaches to getting the H -representation of the local polytope as shown in [BC12]. For the sake of completeness, we will mention them.

Consider the V -representation of the local polytope $L(G)$ corresponding to a graph $G(V, E)$. Removing an edge, say $\{ij\}$ from E is equivalent to removing the corresponding column from the truth-table. Hence, the local polytope $L(G')$ corresponding to $G'(V, E \setminus \{ij\})$ is just the projection of $L(G)$ from $\mathbb{R}^{|V|+|E|}$ onto $\mathbb{R}^{|V|+|E|\setminus\{ij\}}$. This can be achieved by *Fourier-Motzkin elimination*.

Proposition 10.1. *The H -representation of the local polytope for the graph $G'(V, E \setminus \{ij\})$ can be obtained by applying Fourier-Motzkin elimination to remove q_{ij} from the H -representation of the local polytope of the graph $G(V, E)$, and then throwing away the redundant inequalities.*

As an example, let us derive the H -representation of $L(C_4)$ from the H -representation $L(K_4 - e)$ which is given by:

$$\begin{aligned} 0 \leq q_{ij} \leq \min(p_i, p_j) \\ p_i + p_j - p_{ij} \leq 1 \end{aligned} \tag{50}$$

$$p_1 + p_2 + p_3 - q_{12} - q_{23} - q_{13} \leq 1 \tag{51a}$$

$$p_1 + p_3 + p_4 - q_{14} - q_{34} - q_{13} \leq 1 \tag{51b}$$

$$-p_2 + q_{12} + q_{23} - q_{13} \leq 0 \tag{51c}$$

$$-p_4 + q_{14} + q_{34} - q_{13} \leq 0 \tag{51d}$$

$$-p_3 - q_{12} + q_{23} + q_{13} \leq 0 \tag{52a}$$

$$-p_1 - q_{23} + q_{12} + q_{13} \leq 0 \tag{52b}$$

$$-p_3 - q_{14} + q_{34} + q_{13} \leq 0 \tag{52c}$$

$$-p_1 - q_{34} + q_{14} + q_{13} \leq 0 \tag{52d}$$

The equations (50) are the trivial facets corresponding to $N(K_4 - e)$. Equations (51) and (52) are the non-trivial facets for $L(K_4 - e)$ with negative and positive unity as coefficients of q_{13} respectively.

To eliminate q_{13} , we just add the opposite signed inequalities. The resulting set of inequalities will have many redundant inequalities which can be removed by checking against a linear program [BV04]. The minimal set of these inequalities forming the H -representation of $L(K_4 - e)$ are:

| Inequalities of $L(K_4 - e)$ | | Resultant Inequality for $L(C_4)$ |
|------------------------------|-----|---|
| 52a | 51b | $p_1 + p_4 - q_{14} - q_{34} - q_{12} + q_{23} \leq 1$ |
| 52b | 51d | $-p_1 - p_4 + q_{14} + q_{34} + q_{12} - q_{23} \leq 0$ |
| 52b | 51b | $p_3 + p_4 - q_{14} - q_{34} + q_{12} - q_{23} \leq 1$ |
| 52a | 51d | $-p_3 - p_4 + q_{14} + q_{34} - q_{12} + q_{23} \leq 0$ |
| 52c | 51a | $p_1 + p_2 - q_{14} + q_{34} - q_{12} - q_{23} \leq 1$ |
| 52d | 51c | $-p_1 - p_2 + q_{14} - q_{34} + q_{12} + q_{23} \leq 0$ |
| 52d | 51a | $p_2 + p_3 + q_{14} - q_{34} - q_{12} - q_{23} \leq 1$ |
| 52c | 51c | $-p_2 - p_3 - q_{14} + q_{34} + q_{12} + q_{23} \leq 0$ |

TABLE 3. The inequalities of $L(C_4)$ obtained from applying Fourier-Motzkin on inequalities for $L(K_4 - e)$. The first column shows the inequalities which are added to obtain the resultant inequalities in column 2

Aside from these 8 inequalities, the other inequalities in the H -representation of $L(C_4)$ are the 16 inequalities in (50) that do not contain q_{13} . Comparing to Eqs. (30) and (31), we have the complete H -representation of $L(C_4)$.

Thus, from (10.1), if the list of facets of K_n is known, the facets of any subgraph with the same set of vertices can be obtained.

Another approach towards unravelling the H -representation for a graph is the technique of gluing smaller graphs to get a larger graph as shown in [BC12]. For the sake of completeness, we will briefly mention this procedure.

Proposition 10.2. *Consider two graphs $G_1(V_1, E_1)$ and $G_2(V_2, E_2)$ with corresponding H -representations of the local polytope given by $\mathcal{H}_k(p_i \in V_k, q_{ij} \in E_k)$. Now, let the graph formed by gluing G_1 and G_2 on some vertices be $G(V_1 \cup V_2, E_1 \cup E_2)$, such that the induced subgraph on these common vertices is the identical for both graphs. Then, the H -representation of $L(G)$ is the just $\mathcal{H}(p_i \in V_1 \cup V_2, q_{ij} \in E_1 \cup E_2) \equiv \mathcal{H}_1(p_i \in V_1, q_{ij} \in E_1) \cup \mathcal{H}_2(p_i \in V_2, q_{ij} \in E_2)$.*

This is because gluing two graphs in such a way effectively results in a tree structure as shown in (12). As long as the two subgraphs admit a probability assignment and the values at the intersection coincide, the overall tree always admits a joint probability assignment. Thus, studying the geometry of the resulting graph involves studying the geometry of the cartesian product of the subgraphs.



FIGURE 12. The tree structure generated on gluing graphs

As an example, notice that $K_4 - e$ can be formed by gluing two K_3 along an edge. Infact, the two sets of inequalities (51a, 51c, 52a, 52b) and (51b, 51d, 52c, 52d) are isomorphic to (12) over some vertex relabellings. Hence, H -representation of $L(K_4 - e)$ can be obtained from the H -representation of $L(K_3)$.

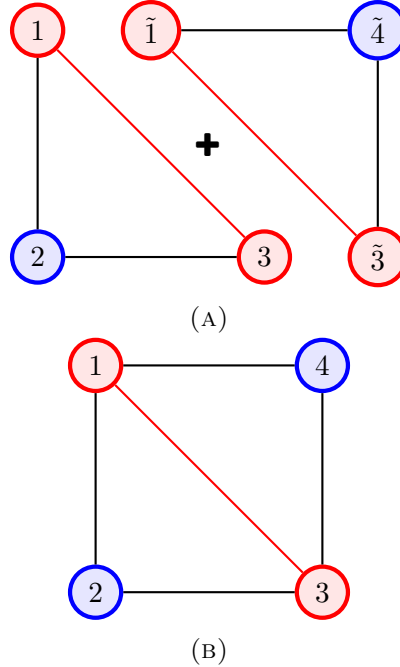


FIGURE 13. $K_4 - e$ formed by joining two K_3 as shown in (A). The red components in (B) show the common induced subgraph.

A direct consequence of (10.1) and (10.2) is that all the non-trivial inequalities (39) for $L(C_n)$ can be obtained just by iteratively gluing together K_3 along an edge and removing it as demonstrated in [AQB⁺13].

Lets start by studying, how Proposition 10.1 and Proposition 10.2 affect the volume ration properties defined at the end of Section 5.

Lemma 10.3. *Consider a graph $G'(V, E \setminus \{ij\})$ obtained by removing an edge from the graph $G(V, E)$. Then, $\tau(G') \geq \tau(G)$.*

Proof. Consider an inequality labeled by k to be written in the form:

$$[v_1 \ v_2 \ \dots \ v_{|V|} \ w_1 \ w_2 \ \dots \ w_{|E|}] \times [p_i \ q_{ij}]^\dagger \leq C_k$$

Let m_k be the number of positive coefficients v_i and n_k be the number of positive coefficients w_i . If this inequality forms the H -representation of $L(G(V, E))$, then for the symmetric slices $p_i = t \ \forall i \in V$, the value of t at which the inequality becomes active is given by $C_k/(m_k + n_k)$.

Now, consider adding two inequalities labelled by 1 and 2, to obtain a new inequality labelled by 3. Then,

$$\begin{aligned} m_3 &\leq m_1 + m_2 \\ n_3 &\leq n_1 + n_2 \\ C_3 &= C_1 + C_2 \end{aligned} \tag{53}$$

This new inequality becomes active at $C_3/(m_3 + n_3)$ and we have,

$$\min \left\{ \frac{C_1}{m_1 + n_1}, \frac{C_2}{m_2 + n_2} \right\} \leq \frac{C_1 + C_2}{m_1 + m_2 + n_1 + n_2} \leq \frac{C_3}{m_3 + n_3} \tag{54}$$

Thus, any inequality obtained as a result of applying Fourier-Motzkin elimination becomes active at t larger than its constituents and (10.3) is implied. \square

Proposition 10.4. *For any graph $G(V, E)$,*

$$\tau(G) \geq \tau(K_{|V|})$$

This follows from (10.3) as any graph with $|V|$ vertices can be formed by iteratively removing edges from $K_{|V|}$.

Proposition 10.5. *Consider a graph $G(V_1 \cup V_2, E_1 \cup E_2)$ formed by gluing two graphs $G_1(V_1, E_1)$ and $G_2(V_2, E_2)$. Then,*

$$\tau(G) = \min\{\tau(G_1), \tau(G_2)\}$$

This follows directly from (10.2) as the set of inequalities in H -representation of G is just the union of set of inequalities in the H -representation of G_1 and G_2 .

Finally in this section we would like to make a conjecture about fall-off value based on the graphs we have studied (see Section 11) and add concluding remarks section.

Conjecture 10.6. *For a graph G of treewidth $\text{tw}(G)$, the fall-off value is given by,*

$$\tau(G) = \frac{1}{\text{tw}(G) + 1}$$

Proposition 10.7. *The facet defining Inclusion-Exclusion inequalities cannot falsify Conjecture 10.6.*

Proof. Consider a complete graph with N vertices with $p_i, i \in \{1, \dots, N\}$ being the probabilities of the corresponding events. Consider an Inclusion-Exclusion inequality for the graph which is formed by the union of n events $p_i, i \in \{1, \dots, n\}$ and k complements $p_{\bar{j}} = 1 - p_j, j \in \{n+1, \dots, N\}$ ($n+k=N$). Such an inequality will be of the form:

$$\sum_{i=1}^n p_i + \sum_{j=n+1}^N p_{\bar{j}} - \sum_{i=1}^n \sum_{j=i+1}^n q_{ij} - \sum_{i=1}^n \sum_{j=n+1}^N q_{i\bar{j}} - \sum_{i=n+1}^N \sum_{j=i+1}^N q_{\bar{i}\bar{j}} \leq 1$$

where q_{ij} is the probability of the intersection of events corresponding to p_i and p_j . Fixing our marginals $p_i = t$ for all $i \in \{1, \dots, N\}$, this inequality becomes:

$$\begin{aligned} & \sum_{i=1}^n t + \sum_{j=n+1}^N (1-t) - \sum_{i=1}^n \sum_{j=i+1}^n q_{ij} - \sum_{i=1}^n \sum_{j=n+1}^N (t - q_{i\bar{j}}) - \sum_{i=n+1}^N \sum_{j=i+1}^N (1 - 2t + q_{\bar{i}\bar{j}}) \leq 1 \\ & nt + k(1-t) - \sum_{i=1}^n \sum_{j=i+1}^n q_{ij} - nkt + \sum_{i=1}^n \sum_{j=n+1}^N q_{ij} - \binom{k}{2}(1-2t) - \sum_{i=n+1}^N \sum_{j=i+1}^N q_{ij} \leq 1 \\ & - \sum_{i=1}^n \sum_{j=i+1}^n q_{ij} - \sum_{i=n+1}^N \sum_{j=i+1}^N q_{ij} + \sum_{i=1}^n \sum_{j=n+1}^N q_{ij} \leq \frac{(k-1)(k-2)}{2} + [(N+3)k - 2k^2 - N]t \end{aligned}$$

Now, the inequality becomes active only when the maximum value of left hand side of the inequality becomes equal to the minimum value of the right hand side. The maximum value of $q_{ij} = t$ for $p_i = p_j = t$. Thus, on simplifying the value of t at which the inequality becomes active is given by:

$$t = -\frac{(k-1)(k-2)}{2(3k - k^2 - N)} \quad (55)$$

We see for $k=1, 2, t=0$. Hence, the the corresponding inequalities distinguish the body L and (N) for small t . The first inequalities to becomes active at non-zero t occur for $k=0, 3$. The corresponding value of $t=1/N$ in accordance to 10.6 for complete graphs. \square

Proposition 10.8. *Conjecture 10.6 holds true for all graphs with 4 or less vertices.*

This simply follows from Proposition 9.1, Proposition 10.7 and the fact that removing an edge from a complete graph lowers the treewidth.

Let us now show that Conjecture 10.6 holds for *series-parallel* graphs, i.e. graphs that have treewidth 2. Note that the Conjecture 10.6 is obviously true for forests (graphs having treewidth 1), since in that case $L(G) = N(G)$, see Proposition 3.8.

Our main tool will be the following result, characterizing the facet structure of $L(G)$, for a series-parallel graph G .

Proposition 10.9 ([Pad89, Theorem 10]). *For any series-parallel graph G , odd-cycle inequalities define all the facets of the local polytope $L(G)$.*

Let us explain next what are odd-cycle inequalities and how to obtain them; our presentation follows closely [Pad89, Section 4]. Let C be a non-trivial, simple cycle of G (seen as a collection of edges) and $M \subseteq C$ a subset of the edges in C of odd cardinality $m := |M|$. If $S \subseteq V$ is the set of vertices incident to the edges in C , we define

$$\begin{aligned} S_0 &:= \{v \in S : \exists e \neq f \in M \text{ with } e \cap f = v\} \\ S_2 &:= \{v \in S : \exists e \neq f \in C \setminus M \text{ with } e \cap f = v\} \\ S_1 &:= S \setminus (S_0 \sqcup S_2). \end{aligned}$$

Then, the *odd-cycle inequality* corresponding to the pair (C, M) is:

$$\sum_{v \in S_0} p_v - \sum_{v \in S_2} p_v - \sum_{e \in M} q_e + \sum_{e \in C \setminus M} q_e \leq \left\lfloor \frac{m}{2} \right\rfloor. \quad (56)$$

Such inequalities are satisfied for all the elements in $L(G)$, see [Pad89]. For example, in the case $G = C = K_3$, taking $M = \{(12)\}$ yields $S_0 = \emptyset$, $S_2 = \{3\}$, and $S_1 = \{1, 2\}$, giving the inequality

$$-p_3 - q_{12} + q_{13} + q_{23} \leq 0,$$

which is the last inequality in Eq. (12). The other inequalities can be obtained by varying the subset M .

Let us now consider the correlation slice corresponding to setting $p_v = t$ for all vertices v of a series-parallel graph. Eq. (56) reads in this case, after the change of variables $q_e \leftarrow tx_e$,

$$\sum_{e \in M} x_e - \sum_{e \in C \setminus M} x_e \geq |S_0| - |S_2| - \frac{\lfloor m/2 \rfloor}{t}. \quad (57)$$

One can easily see that for $m = 1$, the inequality above does not depend on t .

Lemma 10.10. *The inequality (57) is trivially satisfied for all $t \leq 1/3$.*

Proof. Clearly, the minimum possible value of the left-hand-side of (57) is $-|C \setminus M|$. One can easily show that for all C, M , we have [Pad89]

$$|S_0| - |S_2| = |M| - |C \setminus M|.$$

Hence, (57) is trivially satisfied whenever

$$-|C \setminus M| \geq |S_0| - |S_2| - \frac{\lfloor m/2 \rfloor}{t} \iff t \leq \frac{\lfloor m/2 \rfloor}{m}.$$

The latter is an increasing function of m , attaining its minimum $1/3$ for odd m at $m = 3$. \square

We have now all the elements to prove one of our main results.

Theorem 10.11. *Conjecture 10.6 holds for series-parallel graphs G : if $\text{tw}(G) = 2$, then $\tau(G) = 1/3$.*

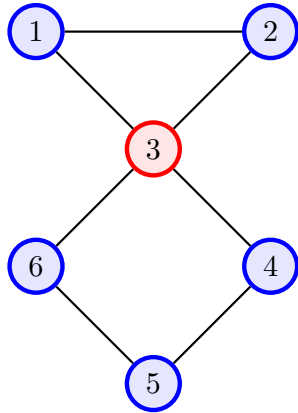
Proof. Let G be a series-parallel graph. By Proposition 10.9, we know that the polytope $L(G)$ is described only by odd-cycle inequalities, which, by the previous lemma, are trivially satisfied for $t \leq 1/3$; hence $\tau(G) \geq 1/3$. Moreover, since $\text{tw}(G) = 2$, G is not a forest, so it contains a cycle. Consider the *smallest* induced subgraph H of G that contains a cycle. The graph H must actually be a cycle, since the presence of extra edges would contradict its minimality. We have shown in Proposition 8.9 that $\tau(H) = 1/3$, so $L(H)$ has a non-trivial facet that becomes “active” at $t = 1/3$. By [Pad89, Corollary 2], the same holds for G ; hence $\tau(G) \leq 1/3$, finishing the proof. \square

We consider the effect of different operations on graphs on the volume ratio of the local and non-signaling polytopes.

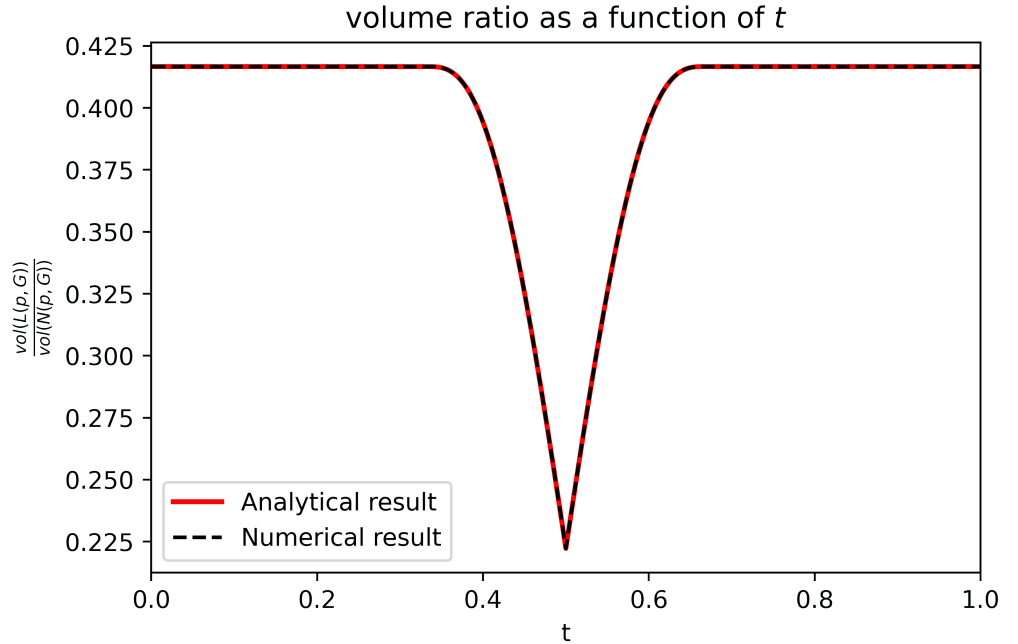
Proposition 10.12. *For two graphs G_1 and G_2 glued together on a single vertex, the resulting G has, for symmetric slices $p = (t, \dots, t)$,*

$$\frac{\text{vol } L(p, G)}{\text{vol } N(p, G)} = \frac{\text{vol } L(p, G_1)}{\text{vol } N(p, G_1)} \times \frac{\text{vol } L(p, G_2)}{\text{vol } N(p, G_2)}$$

As an example, consider the graph in Fig. 14a formed by a product of K_3 and $K_{2,2}$. Its volume ratio can be obtained using Proposition 6.2 and Proposition 7.1. This has been plotted against the numerical results in Fig. 14b.



(A) Graph formed by joining K_3 and $K_{2,2}$ along a vertex



(B) Analytically and numerically calculated ratio of volumes

FIGURE 14

This is because, in terms of the H -representation gluing two graphs along a vertex is just taking the combined set of inequalities for both graphs. Note that these two sets would not have any identical inequalities unlike the case where two graphs are glued along an edge. Hence, the resultant polytope is just the prism product of its constituents whose volume is the product of volumes of its constituents [Man12, TOG17].

Proposition 10.13. *Consider a graph G' obtained by gluing a tree to the graph G . Then,*

$$\frac{\text{vol } \mathbf{L}(p, G')}{\text{vol } \mathbf{N}(p, G')} = \frac{\text{vol } \mathbf{L}(p, G)}{\text{vol } \mathbf{N}(p, G)}$$

Proof. This follows from Proposition 10.5 and Proposition 3.7. □

11. CONCLUSION

Throughout this paper we have studied the geometry of correlation and transportation polytopes by looking at fixed (symmetrical) marginal slices and studying their volume ratios. These bodies are closely related to the non-contextual and no-disturbance polytopes which are of prime interest in Quantum Foundations.

The characterization of the volume ratio for trees (treewidth = 1) is trivial. We provide a complete analysis for the K_3 and $K_{2,2}$ case which famously appear in literature as the Bell-Wigner and CHSH polytopes. We then generalize our analysis to all cyclic graphs. Finally, we also prove theorems on the nature of volume-ratio for all graphs of treewidth two. For graphs with three-width 3, the example of K_4 is worked out explicitly and additional examples are given in the appendices.

Over the course of our analysis, we observe that the volume ratio remains constant for some initial range of the fixed marginal before it starts decreasing and reaches a minimum value. In order to quantify this remarkable fact, we look at parameters such as *fall-off value*, *initial-ratio* and *middle-ratio*. We conjecture that the fall-off value depends on inversely on $\text{tw}(G) + 1$. We then show that this holds in general for treewidth 1 and 2 and holds specifically for some graphs of higher treewidths. To prove the result for a general graph, we need a general way to characterize all facets of a correlation polytopes (or equivalently a cut-polytope). This is a long-standing problem in literature and results exists only for graphs with up to 7 vertices [Gri90].

Contextual correlations are of particular importance in quantum information theory as they are required to obtain advantage over classical information processing protocols [SSW18, SB⁺23, WBG24]. Thus, it is important to realize scenarios/games where a random sampling yields a contextual behaviour. Through our work, we have showed that in scenarios where n -parties are involved in a contextual scenario with contexts of maximum size 2 and the constraint that the single-variable marginal for each party is fixed, the highest chance of getting a contextual correlation with random sampling is possible when the fixed marginals are all $1/2$. What is interesting is fixing the marginals in a clever way can infact increase the odds of getting contextual correlations. For example, consider the CHSH case. When all the probabilities are free, there is a 1 in 17 chance, that a sampled behaviour is contextual. However, once the marginals are fixed to t , the odds can be reduced to $1/3$ when $t = 1/2$. We already saw the significance of the $t = 1/2$ slice for the CHSH case in Section 7. For any general bell game as well, these slices are of importance as they correspond to the players sharing a locally maximally entangled state often linked to maximal quantum violations of local inequalities such as the mermin inequalities [Mer90] where the n -GHZ states are used.

There is scope for a lot of future work in this direction. Analysis for larger contexts, and poly-variate correlations would offer better insight one the distribution of useful correlation boxes in general scenario. Moreover, it would be interesting to relate the ratio of volumes we consider in this paper to other measures of non-contextuality for scenarios encoded by graphs, such as the contextual fraction [ABM17, KD19].

Acknowledgments. I.N. was supported by the ANR projects [ESQuisses](#), grant number ANR-20-CE47-0014-01, and [STARS](#), grant number ANR-20-CE40-0008, as well as by the PHC program *Star* (Applications of random matrix theory and abstract harmonic analysis to quantum information theory). A.K.J. received support from the [French Embassy in India](#) through the [French Excellence Charpak Lab Scholarship](#) Programme.

REFERENCES

- [ABM17] Samson Abramsky, Rui Soares Barbosa, and Shane Mansfield. Contextual fraction as a measure of contextuality. *Physical review letters*, 119(5):050504, 2017. [36](#)
- [AFLS15] Antonio Acín, Tobias Fritz, Anthony Leverrier, and Ana Belén Sainz. A combinatorial approach to nonlocality and contextuality. *Communications in Mathematical Physics*, 334:533–628, 2015. [10](#)
- [AGR82] Alain Aspect, Philippe Grangier, and Gérard Roger. Experimental realization of einstein-podolsky-rosen-bohm gedankenexperiment: A new violation of bell’s inequalities. *Phys. Rev. Lett.*, 49:91–94, 7 1982. [1](#), [8](#)
- [AQB⁺13] Mateus Araújo, Marco Túlio Quintino, Costantino Budroni, Marcelo Terra Cunha, and Adán Cabello. All noncontextuality inequalities for the n-cycle scenario. *Physical Review A*, 88(2):022118, 2013. [25](#), [26](#), [32](#)
- [BC12] Costantino Budroni and Adan Cabello. Bell inequalities from variable-elimination methods. *Journal of Physics A: Mathematical and Theoretical*, 45(38):385304, 2012. [30](#), [31](#)
- [BCP⁺14] Nicolas Brunner, Daniel Cavalcanti, Stefano Pironio, Valerio Scarani, and Stephanie Wehner. Bell nonlocality. *Reviews of modern physics*, 86(2):419, 2014. [1](#)
- [Bel64] John S Bell. On the Einstein Podolsky Rosen paradox. *Physics Physique Fizika*, 1(3):195, 1964. [1](#), [8](#)
- [BM10] Costantino Budroni and Giovanni Morchio. The extension problem for partial boolean structures in quantum mechanics. *Journal of mathematical physics*, 51(12), 2010. [7](#)
- [BV04] Stephen Boyd and Lieven Vandenberghe. *Convex optimization*. Cambridge university press, 2004. [31](#)
- [Cab05] Adán Cabello. How much larger quantum correlations are than classical ones. *Physical Review A*, 72(1):012113, 2005. [2](#), [3](#)
- [CF12] Rafael Chaves and Tobias Fritz. Entropic approach to local realism and noncontextuality. *Physical Review A*, 85(3):032113, 2012. [10](#)
- [CHSH69] John F Clauser, Michael A Horne, Abner Shimony, and Richard A Holt. Proposed experiment to test local hidden-variable theories. *Physical review letters*, 23(15):880, 1969. [1](#), [3](#), [8](#), [20](#)
- [Chu41] Kai Lai Chung. On the probability of the occurrence of at least m events among n arbitrary events. *The Annals of Mathematical Statistics*, 12(3):328–338, 1941. [29](#)
- [CSW14] Adán Cabello, Simone Severini, and Andreas Winter. Graph-theoretic approach to quantum correlations. *Physical review letters*, 112(4):040401, 2014. [10](#)
- [DBAC18] Cristhiano Duarte, Samurá Brito, Barbara Amaral, and Rafael Chaves. Concentration phenomena in the geometry of bell correlations. *Physical Review A*, 98(6):062114, 2018. [2](#)
- [DL94a] Michel Deza and Monique Laurent. Applications of cut polyhedra—i. *Journal of Computational and Applied Mathematics*, 55(2):191–216, 1994. [5](#)
- [DL94b] Michel Deza and Monique Laurent. Applications of cut polyhedra—ii. *Journal of Computational and Applied Mathematics*, 55(2):217–247, 1994. [5](#)
- [Fin82] Arthur Fine. Hidden variables, joint probability, and the bell inequalities. *Physical Review Letters*, 48(5):291, 1982. [9](#), [10](#)
- [Fré51] Maurice Fréchet. Sur les tableaux de corrélation dont les marges sont données. *Ann. Univ. Lyon, 3^e série, Sciences, Sect. A*, 14:53–77, 1951. [4](#)
- [Fuk23] K. Fukuda. `cddlib` – a C implementation of the Double Description Method of Motzkin et al. <https://github.com/cddlib/cddlib>, 2023. [16](#), [29](#)
- [GGLPV17] Carlos E González-Guillén, Cécilia Lancien, Carlos Palazuelos, and Ignacio Villanueva. Random quantum correlations are generically non-classical. *Annales Henri Poincaré*, 18:3793–3813, 2017. [2](#)
- [GJ00] Evgenij Gawrilow and Michael Joswig. Polymake: a framework for analyzing convex polytopes. In *Polytopes—combinatorics and computation*, pages 43–73. Springer, 2000. [40](#)
- [Gri90] Viatcheslav P Grishukhin. All facets of the cut cone cn for $n=7$ are known. *European Journal of Combinatorics*, 11(2):115–117, 1990. [36](#)
- [HBD⁺15] Bas Hensen, Hannes Bernien, Anaïs E Dréau, Andreas Reiserer, Norbert Kalb, Machiel S Blok, Just Ruitenberg, Raymond FL Vermeulen, Raymond N Schouten, Carlos Abellán, et al. Loophole-free bell inequality violation using electron spins separated by 1.3 kilometres. *Nature*, 526(7575):682–686, 2015. [1](#), [8](#)
- [Hoe40] Wassilij Hoeffding. Masstabinvariante korrelationstheorie. *Schriften des Mathematischen Instituts und Instituts für Angewandte Mathematik der Universität Berlin*, 5:181–233, 1940. [4](#)
- [KCBS08] Alexander A Klyachko, M Ali Can, Sinem Binicioğlu, and Alexander S Shumovsky. Simple test for hidden variables in spin-1 systems. *Physical review letters*, 101(2):020403, 2008. [3](#), [25](#)
- [KD19] Janne V Kujala and Ehtibar N Dzhafarov. Measures of contextuality and non-contextuality. *Philosophical Transactions of the Royal Society A*, 377(2157):20190149, 2019. [36](#)

- [KLS97] Chun-Wa Ko, Jon Lee, and Einar Steingrímsson. The volume of relaxed boolean-quadric and cut polytopes. *Discrete Mathematics*, 163(1-3):293–298, 1997. [3](#), [11](#)
- [KLT20] Marek Kaluba, Benjamin Lorenz, and Sascha Timme. Polymake. jl: A new interface to polymake. In *International Congress on Mathematical Software*, pages 377–385. Springer, 2020. [40](#)
- [LMS⁺23] Thinh P Le, Chiara Meroni, Bernd Sturmfels, Reinhard F Werner, and Timo Ziegler. Quantum correlations in the minimal scenario. *Quantum*, 7:947, 2023. [20](#)
- [LS20] Jon Lee and Daphne Skipper. Volume computation for sparse boolean quadric relaxations. *Discrete Applied Mathematics*, 275:79–94, 2020. [3](#), [11](#), [12](#), [22](#), [27](#)
- [Man12] Henry P Manning. *The Fourth Dimension Simply Explained*. Courier Corporation, 2012. [35](#)
- [Mer90] N David Mermin. Extreme quantum entanglement in a superposition of macroscopically distinct states. *Physical Review Letters*, 65(15):1838, 1990. [36](#)
- [Pad89] Manfred Padberg. The boolean quadric polytope: some characteristics, facets and relatives. *Mathematical programming*, 45:139–172, 1989. [3](#), [8](#), [11](#), [34](#), [35](#)
- [Pit86] Itamar Pitowsky. The range of quantum probability. *Journal of Mathematical Physics*, 27(6):1556–1565, 1986. [2](#), [5](#)
- [Pit89a] Itamar Pitowsky. Classical correlation polytopes and propositional logic. *Quantum Probability—Quantum Logic*, pages 11–51, 1989. [12](#)
- [Pit89b] Itamar Pitowsky. From george boole to john bell—the origins of bell’s inequality. In *Bell’s Theorem, Quantum Theory and Conceptions of the Universe*, pages 37–49. Springer, 1989. [12](#)
- [Pit89c] Itamar Pitowsky. *Quantum probability-quantum logic*, volume 321. Springer, 1989. [3](#)
- [Pit91] Itamar Pitowsky. Correlation polytopes: their geometry and complexity. *Mathematical Programming*, 50:395–414, 1991. [5](#), [6](#), [28](#), [29](#)
- [PR94] Sandu Popescu and Daniel Rohrlich. Quantum nonlocality as an axiom. *Foundations of Physics*, 24(3):379–385, 1994. [1](#), [25](#)
- [PV16] Carlos Palazuelos and Thomas Vidick. Survey on nonlocal games and operator space theory. *Journal of Mathematical Physics*, 57(1):015220, 2016. [8](#)
- [SB⁺23] Jaskaran Singh, Rajendra Singh Bhati, et al. No contextual advantage in nonparadoxical scenarios of the two-state vector formalism. *Physical Review A*, 107(1):012206, 2023. [36](#)
- [Sca19] Valerio Scarani. *Bell nonlocality*. Oxford University Press, 2019. [1](#), [10](#)
- [SSW18] David Schmid, Robert W Spekkens, and Elie Wolfe. All the noncontextuality inequalities for arbitrary prepare-and-measure experiments with respect to any fixed set of operational equivalences. *Physical Review A*, 97(6):062103, 2018. [36](#)
- [TOG17] Csaba D Toth, Joseph O’Rourke, and Jacob E Goodman. *Handbook of discrete and computational geometry*. CRC press, 2017. [35](#)
- [WBG24] Rafael Wagner, Rui Soares Barbosa, and Ernesto F Galvão. Inequalities witnessing coherence, nonlocality, and contextuality. *Physical Review A*, 109(3):032220, 2024. [36](#)
- [Wig97] Eugene P Wigner. On hidden variables and quantum mechanical probabilities. *Part I: Particles and Fields. Part II: Foundations of Quantum Mechanics*, pages 515–523, 1997. [12](#)
- [Zie12] Günter M Ziegler. *Lectures on polytopes*, volume 152. Springer Science & Business Media, 2012. [6](#)

APPENDIX A. GRAPHS AND PLOTS

In this appendix, we provide numerical computations of the volume ratio for symmetric slices of different graphs.

A.1. Graphs with 4 vertices. We start with graphs on 4 vertices.

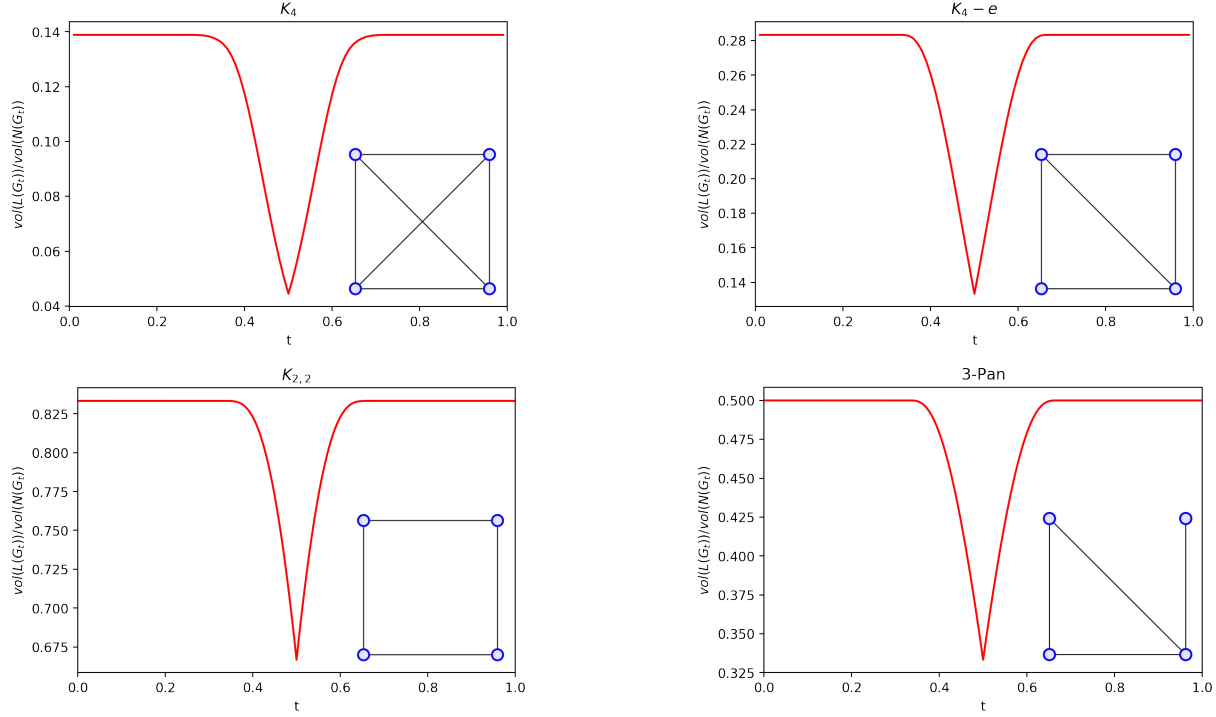


FIGURE 15. Plots of volume ratio of symmetric slices given by, $\text{vol}(\mathbb{L}(p = (t, t, t, t), G)) / \text{vol}(\mathbb{N}(p = (t, t, t, t), G))$ as a function of t for different graphs with 4 vertices. The graphs are shown on the lower right corner of each plot.

| Graph G | $\text{tw}(G)$ | $\tau(G)$ | $\rho_{0+}(G)$ | $\rho_{1/2}(G)$ |
|-----------|----------------|---------------|-----------------|-----------------|
| K_4 | 3 | $\frac{1}{4}$ | $\frac{5}{36}$ | $\frac{2}{45}$ |
| $K_4 - e$ | 2 | $\frac{1}{3}$ | $\frac{17}{60}$ | $\frac{2}{15}$ |
| $K_{2,2}$ | 2 | $\frac{1}{3}$ | $\frac{5}{6}$ | $\frac{2}{3}$ |
| pan | 2 | $\frac{1}{3}$ | $\frac{1}{2}$ | $\frac{1}{3}$ |

TABLE 4. List of parameters for graphs with 4 vertices: treewidth of the graph $\text{tw}(G)$, the threshold $\tau(G)$ until which the volume ratio is constant, the initial (constant) volume ration $\rho_{0+}(G)$, the volume ration at $p = 1/2$, $\rho_{1/2}(G)$.

From Table 4 we see that Conjecture 10.6 holds for all graphs with 4 vertices.

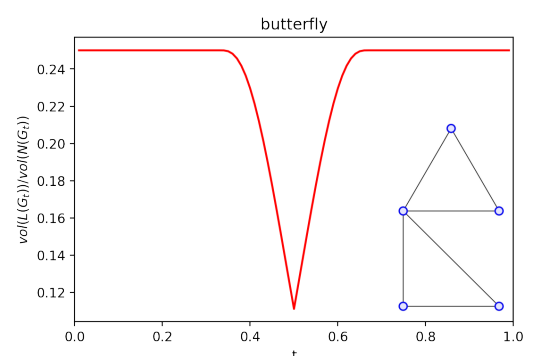
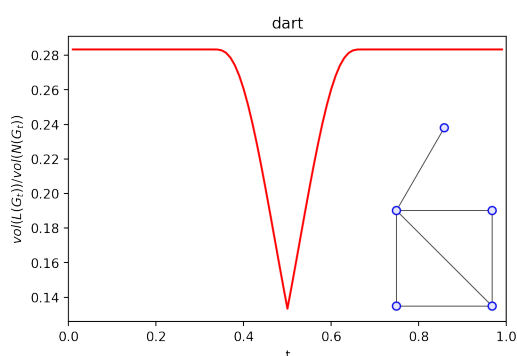
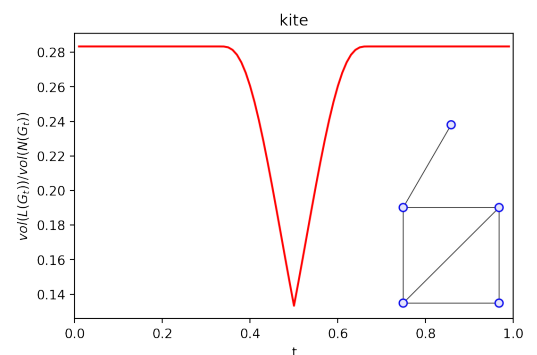
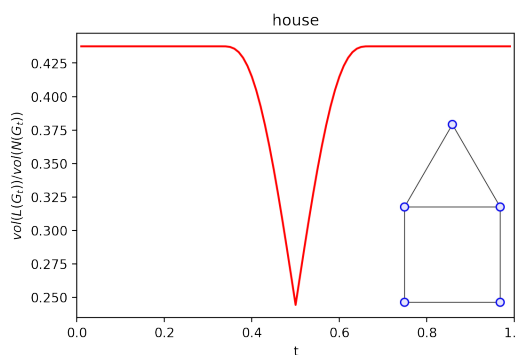
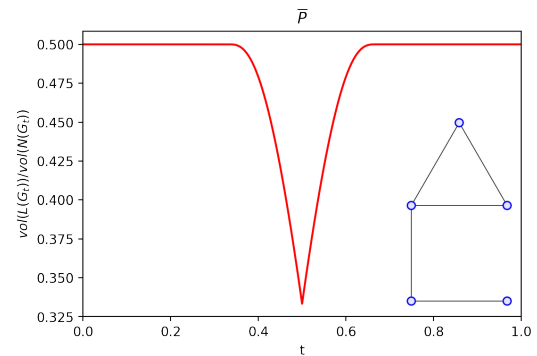
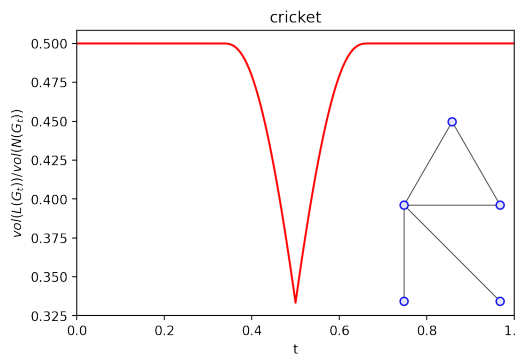
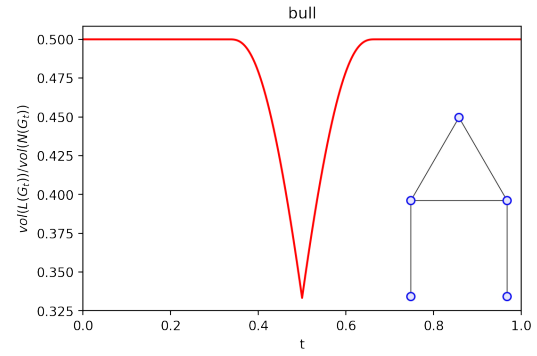
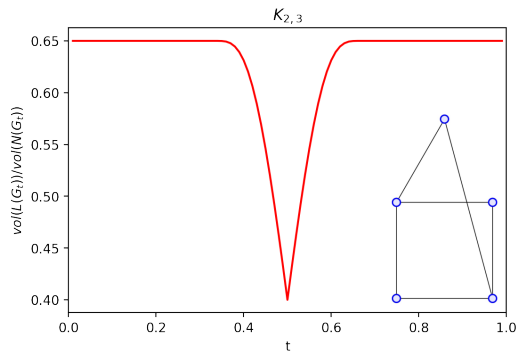
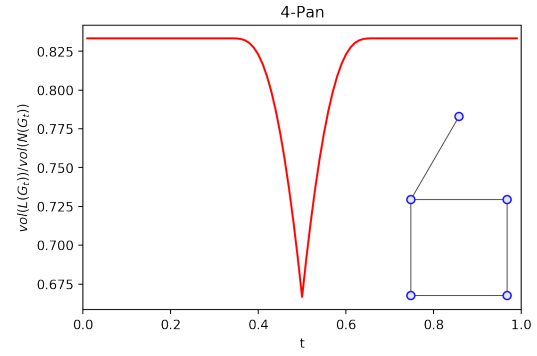
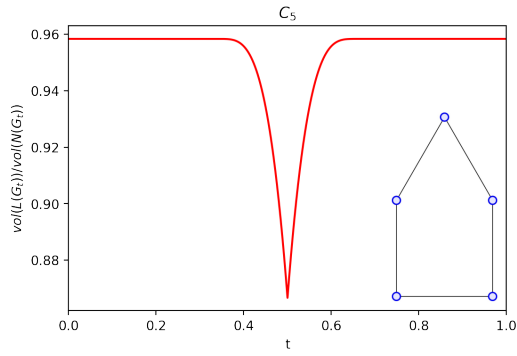
A.2. Graphs with 5 vertices. Next, we give the numerical results for graphs with 5 vertices. Again we see from Table 5 that Conjecture 10.6 holds for all graphs with 5 vertices.

Email address: ion.nechita@univ-tlse3.fr

LABORATOIRE DE PHYSIQUE THÉORIQUE, UNIVERSITÉ DE TOULOUSE, CNRS, UPS, FRANCE

| Graph G | $\text{tw}(G)$ | $\tau(G)$ | $\rho_{0+}(G)$ | $\rho_{1/2}(G)$ |
|-------------------------|----------------|---------------|------------------------|--------------------|
| C_5 | 2 | $\frac{1}{3}$ | $\frac{23}{24}$ | $\frac{13}{15}$ |
| 4-Pan | 2 | $\frac{1}{3}$ | $\frac{5}{6}$ | $\frac{2}{3}$ |
| $K_{2,3}$ | 2 | $\frac{1}{3}$ | $\frac{13}{20}$ | $\frac{2}{5}$ |
| bull/cricket/ \bar{P} | 2 | $\frac{1}{3}$ | $\frac{1}{2}$ | $\frac{1}{3}$ |
| house | 2 | $\frac{1}{3}$ | $\frac{7}{16}$ | $\frac{11}{45}$ |
| kite/dart | 2 | $\frac{1}{3}$ | $\frac{17}{60}$ | $\frac{2}{15}$ |
| butterfly | 2 | $\frac{1}{3}$ | $\frac{1}{4}$ | $\frac{1}{9}$ |
| $P_2 \cup P_3$ | 3 | $\frac{1}{4}$ | $\frac{307}{1260}$ | $\frac{2}{21}$ |
| $K_3 \cup 2K_1$ | 2 | $\frac{1}{3}$ | $\frac{47}{280}$ | $\frac{2}{35}$ |
| gem | 2 | $\frac{1}{3}$ | $\frac{271}{1680}$ | $\frac{17}{315}$ |
| claw $\cup K_1$ | 3 | $\frac{1}{4}$ | $\frac{5}{36}$ | $\frac{2}{45}$ |
| W_4 | 3 | $\frac{1}{4}$ | $\frac{229}{2240}$ | $\frac{8}{315}$ |
| $P_3 \cup K_1$ | 3 | $\frac{1}{4}$ | $\frac{1657}{20160}$ | $\frac{2}{105}$ |
| $K_5 - e$ | 3 | $\frac{1}{4}$ | $\frac{1049}{24192}$ | $\frac{4}{567}$ |
| K_5 | 4 | $\frac{1}{5}$ | $\frac{14731}{725760}$ | $\frac{32}{14175}$ |

TABLE 5. List of parameters for graphs with 5 vertices: treewidth of the graph $\text{tw}(G)$, the threshold $\tau(G)$ until which the volume ratio is constant, the initial (constant) volume ration $\rho_{0+}(G)$, the volume ration at $p = 1/2$, $\rho_{1/2}(G)$. The volume computations are obtained using a Julia package [KLT20] for Polymake [GJ00].



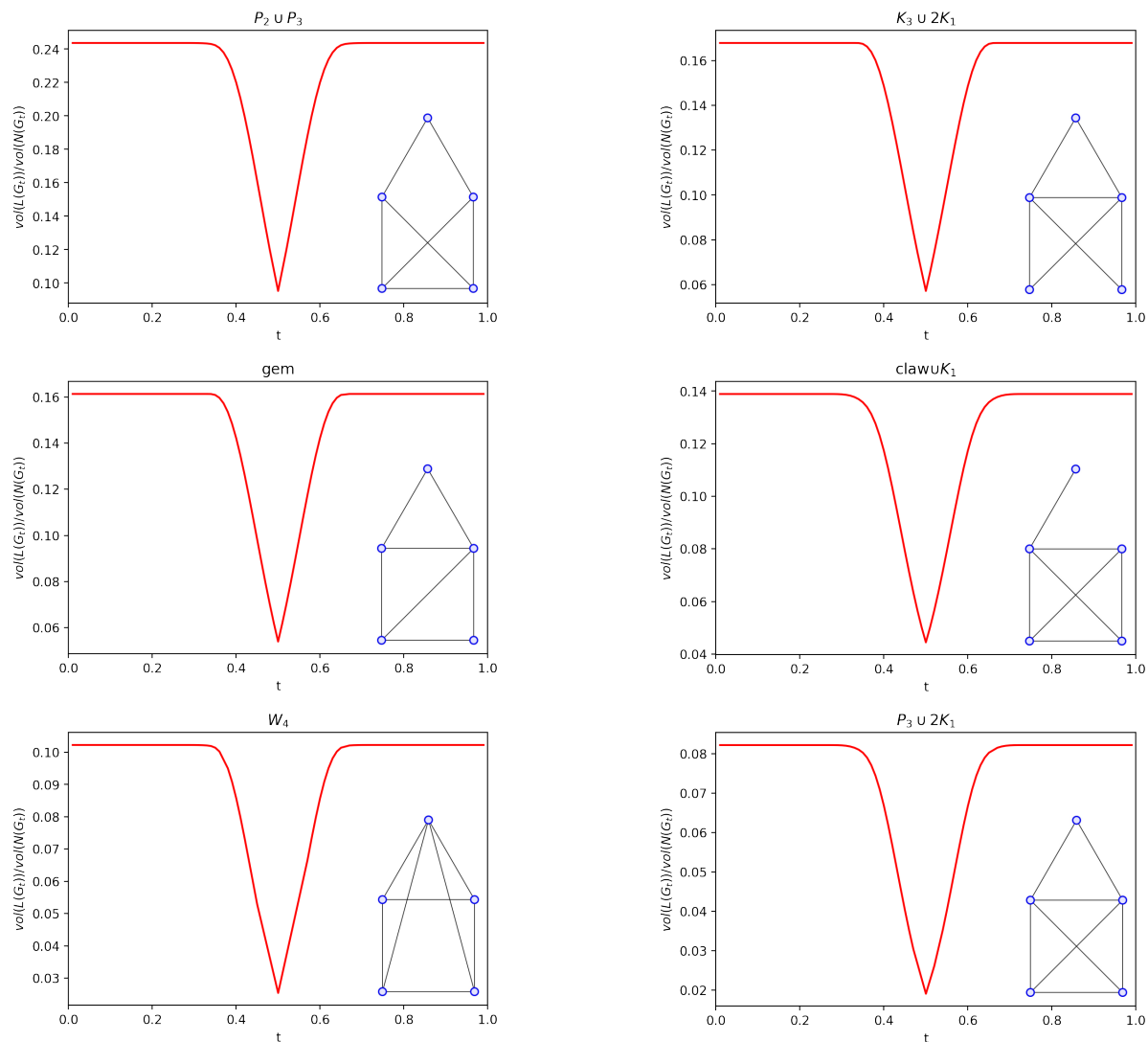


FIGURE 16. Plots of volume ratio of symmetric slices given by $\text{vol}(\mathbb{L}(p = (t, t, t, t, t), G)) / \text{vol}(\mathbb{N}(p = (t, t, t, t, t), G))$ as a function of t for different graphs with 5 vertices. The graphs are displayed on the lower right corner of each plot. The plots for graphs $K_5 - e$ and K_5 are excluded due to computational intractability.